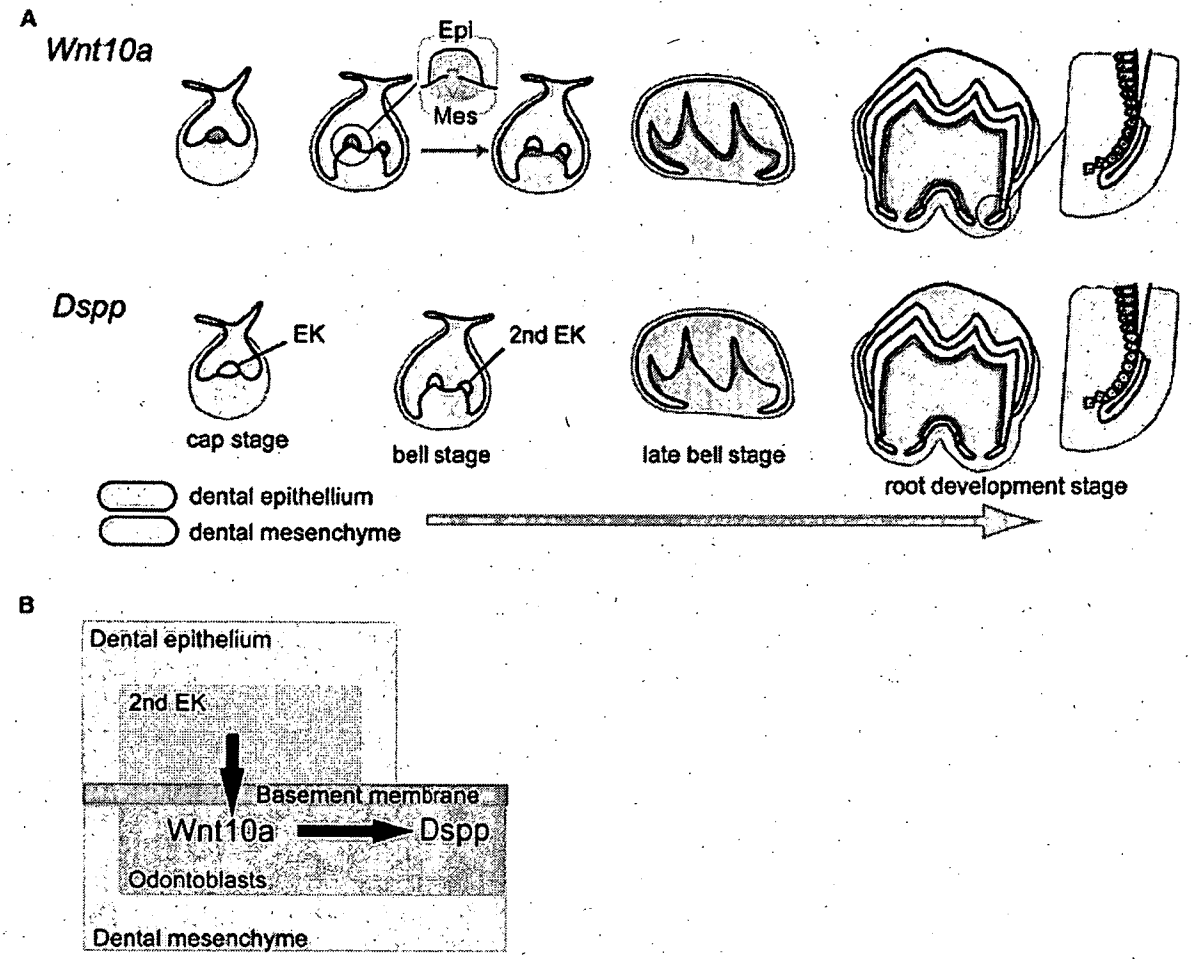

Fig. 6 (A) Summary of the expression of *Wnt10a* and *Dspp* during tooth development. *Wnt10a* is expressed in the enamel knot (EK) at the cap stage. At the bell stage, *Wnt10a* is expressed in the secondary enamel knot (2nd EK), and the expression has shifted to the underlying mesenchyme. In the late bell stages, *Wnt10a* expression is continuous in the preodontoblasts and odontoblasts. *Dspp* is expressed in the odontoblasts in the cusp regions. During root development, both *Wnt10a* and *Dspp* expression domains overlap in the odontoblasts. However, *Wnt10a* expression appeared earlier in the differentiating preodontoblasts underlying the epithelial root sheath. (B) Schematic diagram illustrating induction of *Dspp* expression by Wnt10a signals in the odontoblast cell lineage. *Wnt10a* appears in the mesenchymal cells beneath the secondary enamel knots. Wnt10a induces *Dspp* expression in the odontoblasts, and cell to matrix interactions are required for the induction of *Dspp* expression by Wnta10a. Hence, Wnt10a links tooth morphogenesis and odontoblast differentiation.

mesenchymal cells and the basement membrane underlining the enamel epithelium (Thesleff and Hurmerinta, 1981). Many extracellular matrix molecules were implicated in the cell–matrix interactions including fibronectin and other glycoproteins as well as proteoglycans. It was also suggested that growth factors and other diffusible molecules may have been trapped in the basement membrane, and involved in communication between cells. Interestingly, *Dspp* was induced only when the *Wnt10a*-transfected cells were cultured on Matrigel, which is an extract of basement membrane proteins (Kleinman et al., 1982), supporting the idea that cell to matrix association plays some role in odontoblast differentiation. As Mock-transfected cell did not show *Dspp* expression on Matrigel, Matrigel itself cannot induce odontogenesis. Among various molecules in the basement membrane, laminin alfa2 is subunit of laminin-2. Laminin-α2 deficiency resulted in a dramatic decrease in *Dspp* expression in odontoblasts (Yuasa et al., 2004), which is in agreement with our data and also supports the idea that cell–matrix interaction is essential for Dspp expression.

Heparan sulfate proteoglycans are major components of the extracellular matrix and regulate the transmission of developmental signals (Hacker et al., 2005). They also modulate the Wnt pathway (Haerry et al., 1997). In tooth development, odontoblast differentiation was inhibited *in vitro* by tunicamycin, which inhibited protein glycosylation and the accumulation of proteoglycans and glycoproteins in the basement mem-

brane of the developing tooth (Thesleff and Pratt, 1980). In tooth development also the cell surface proteoglycan syndecan-1 is involved in epithelial–mesenchymal interactions (Vainio et al., 1989; Thesleff et al., 1991), and syndecan-3 has been detected in the odontoblast layer underlying the inner enamel epithelium (Hikake et al., 2003). Heparin-sulfated forms of proteoglycans (HSPG) are long proteins with branched sugar side chains that are expressed on the cell surface, and can form complexes with a variety of signaling molecules, including Wnts and fibroblast growth factors (Nybakken and Perrimon, 2002). Hence it is possible that Wnt10a can be captured in the basement membrane extracellular matrix molecules to control differentiation of the pulp cells into odontoblasts. In addition, spatial distribution patterns of *Wnt10a* mRNA expression, together with previous findings, might provide an insight into a possible association between Wnt signaling and heparan sulfate proteoglycan in dentinogenesis. With tooth development, the basement membrane degrades and odontoblasts come into contact with the predentin surface. As predentin also contains various extracellular matrix molecules, such as proteoglycan and fibronectin (Linde and Goldberg, 1993), the cell–matrix interaction between odontoblasts and predentin might thus be explained the continuous expression of Wnt10a and Dspp in odontoblasts after the basement membrane has disappeared.

In our study, transfected cells were cultured on Matrigel in the medium supplemented with serum. Although both serum and Matrigel contain many growth factors and proteins these did not induce odontoblast differentiation as shown by the lack of *Dspp* expression in Mock transfected cells. Our real-time PCR data demonstrated that the *Dspp* induction by forced overexpression of *Wnt10a* was specific.

Odontoblast differentiation is regulated by reciprocal epithelial mesenchymal interactions. In addition, Dspp is expressed in a time- and site-specific manner and Dspp-expressing odontoblasts lie in one cell layer. These findings suggest that Dspp expression could be regulated by several inhibitory and stimulatory factors in a coordinated manner. Our real-time PCR data showed that Dspp induction in Wnt10a transfected-non-odontogenic cells was much less than the Dspp expression in intact odontoblasts. These data suggested that Wnt10a thus plays an important role in Dspp induction, however, further interaction with other putative molecules might be necessary to express a sufficient amount of Dspp during odontoblast differentiation.

Wnt10a and tooth morphogenesis

In the early tooth, *Wnt10a* is expressed in the enamel knot (Dassule and McMahon, 1998), which has a central function in the control of growth and patterning of the tooth crown (Jernvall and Thesleff, 2000; Miletich and Sharpe, 2003). Our *in situ* hybridization analysis showed that *Wnt10a* expression was reiterated in the secondary enamel knots which express most of the same signal molecules as the primary enamel knots and initiate cusp formation (Fig. 6A) (Vaahtokari et al., 1996). Interestingly, we found that *Wnt10a* expression shifted from the secondary enamel knots to the underlying mesenchyme. It could be that mesenchymal *Wnt10a* expression was induced by signaling molecules of the secondary enamel knots, perhaps by Wnt10a itself. The continuous *Wnt10a* mRNA distribution pattern in the odontoblasts suggested autocrine regulation of *Wnt10a* expression in the mesenchymal cells after the initial induction of *Wnt10a* by the epithelium.

Our study has provided new insight into the molecular mechanisms that spatially and temporally control the initiation of odontoblast differentiation. The terminal differentiation of odontoblasts is initiated at the tip of each cusp, indicating that the cell fate decision and morphogenesis is tightly linked (Fig. 6B). As both the initiation of odontoblast differentiation and the initiation of cusps coincide temporally and spatially with the secondary enamel knots, and as both processes are induced by epithelial signals (Jernvall et al., 1994; Jernvall and Thesleff, 2000), it is conceivable that some signals could regulate both cell differentiation as cusp morphogenesis. Our observations indicated that the expression of Wnt10a was intimately linked with the secondary enamel knots and the gradient of cytodifferentiation propagating apically from each cusp tip. Our data clearly demonstrated that *Wnt10a*-shifting from the epithelial signaling center to the underlying mesenchyme temporally and spatially corresponds to the initiation of odontoblast differentiation. In addition, functional network of Wnt10a and the cell to matrix interactions may trigger and regulate tooth specific *Dspp* expression. Putative matrix molecules may provide the cues for polarization of the cells, which may be necessary also for the transmission of the Wnt10a signal from the epithelium to the preodontoblast.

In summary, we found that *Wnt10a* was specifically expressed in the odontoblast cell lineage in mouse molars with striking colocalization with *Dspp* mRNA expression in the fully differentiated secretory odontoblasts. Dspp is a key molecule for dentin mineralization, and we showed that the forced expression of *Wnt10a* induced *Dspp* mRNA in pluripotent fibroblast cells, indicating that Wnt10a is possibly involved in dentine mineralization as an upstream regulator of Dspp. However, our observation that *Dspp* was induced only when the transfected cells were cultured on Matrigel suggests that cell to matrix interactions have crucial roles in dentinogenesis in conjunction with Wnt10a. This supports earlier proposals that odontoblast differentiation requires interactions between the mesenchymal cells and the extracellular matrix. We also found

that *Wnt10a* was expressed in the epithelial secondary enamel knots, and that this expression shifted to the underlying mesenchymal cells. The timing and location of this shift corresponds to the initiation of the polarization of preodontoblasts. Taken together, our findings indicate that Wnt10a and cell to matrix interactions play an important role for odontoblast differentiation and that Wnt10a links tooth morphogenesis and the differentiation of odontoblasts.

Acknowledgments We thank Merja Mäkinen and Riikka Santalahti for their excellent technical assistance. This study was supported by Grants-in-Aid for Scientific Research from the Japan Society for the Promotion of Science, the Academy of Finland, and the Sigrid Juselius Foundation.

References

Åberg, T., Wozney, J. and Thesleff, I. (1997) Expression patterns of bone morphogenetic proteins (Bmps) in the developing mouse tooth suggest roles in morphogenesis and cell differentiation. Dev Dyn 210:383–396.

Asahina, I., Sampath, T.K. and Hauschka, P.V. (1996) Human osteogenic protein-1 induces chondroblastic, osteoblastic, and/or adipocytic differentiation of clonal murine target cells. Exp Cell Res 222:38–47.

Bennett, C.N., Longo, K.A., Wright, W.S., Suva, L.J., Lane, T.F., Hankenson, K.D. and MacDougald, O.A. (2005) Regulation of osteoblastogenesis and bone mass by Wnt10b. Proc Natl Acad Sci USA 102:3324–3329.

Bleicher, F., Couble, M.L., Farges, J.C., Couble, P. and Magloire, H. (1999) Sequential expression of matrix protein genes in developing rat teeth. Matrix Biol 18:133–143.

Cadigan, K.M. and Nusse, R. (1997) Wnt signaling: a common theme in animal development. Genes Dev 11:3286–3305.

Dassule, H.R. and McMahon, A.P. (1998) Analysis of epithelial–mesenchymal interactions in the initial morphogenesis of the mammalian tooth. Dev Biol 202:215–227.

D'Souza, R.N., Cavender, A., Sunavala, G., Alvarez, J., Ohshima, T., Kulkarni, A.B. and MacDougall, M. (1997) Gene expression patterns of murine dentin matrix protein 1 (Dmp1) and dentin sialophosphoprotein (DSPP) suggest distinct developmental functions in vivo. J Bone Miner Res 12:2040–2049.

Feng, J.Q., Luan, X., Wallace, J., Jing, D., Ohshima, T., Kulkarni, A.B., D'Souza, R.N., Kozak, C.A. and MacDougall, M. (1998) Genomic organization, chromosomal mapping, and promoter analysis of the mouse dentin sialophosphoprotein (Dspp) gene, which codes for both dentin sialoprotein and dentin phosphoprotein. J Biol Chem 273:9457–9464.

Hacker, U., Nybakken, K. and Perrimon, N. (2005) Heparan sulphate proteoglycans: the sweet side of development. Nat Rev Mol Cell Biol 6:530–541.

Haerry, T.E., Heslip, T.R., Marsh, J.L. and O'Connor, M.B. (1997) Defects in glucuronate biosynthesis disrupt Wingless signaling in Drosophila. Development 124:3055–3064.

Hartmann, C. (2006) A Wnt canon orchestrating osteoblastogenesis. Trends Cell Biol 16:151–158.

Hikake, T., Mori, T., Iseki, K., Hagino, S., Zhang, Y., Takagi, H., Yokoya, S. and Wanaka, A. (2003) Comparison of expression patterns between CREB family transcription factor OASIS and proteoglycan core protein genes during murine tooth development. Anat Embryol (Berlin) 206:373–380.

James, M.J., Jarvinen, E. and Thesleff, I. (2004) Bonol: a gene associated with regions of deposition of bone and dentine. Gene Expr Patterns 4:595–599.

Jernvall, J., Kettunen, P., Karavanova, I., Martin, L.B. and Thesleff, I. (1994) Evidence for the role of the enamel knot as a control center in mammalian tooth cusp formation: non-dividing cells express growth stimulating Fgf-4 gene. Int J Dev Biol 38:463–469.

Jernvall, J. and Thesleff, I. (2000) Reiterative signaling and patterning during mammalian tooth morphogenesis. Mech Dev 92:19–29.

Katagiri, T., Yamaguchi, A., Ikeda, T., Yoshiki, S., Wozney, J.M., Rosen, V., Wang, E.A., Tanaka, H., Omura, S. and Suda, T. (1990) The non-osteogenic mouse pluripotent cell line, C3H10T1/2, is induced to differentiate into osteoblastic cells by recombinant human bone morphogenetic protein-2. Biochem Biophys Res Commun 172:295–299.

Kleinman, H.K., McGarvey, M.L., Liotta, L.A., Robey, P.G., Tryggvason, K. and Martin, G.R. (1982) Isolation and characterization of type IV procollagen, laminin, and heparan sulfate proteoglycan from the EHS sarcoma. Biochemistry 21: 6188–6193.

Kollar, E.J. (1985) Tissue interactions in development of teeth and related ectodermal derivatives. Dev Biol (NewYork) 4: 297–313.

Kratochwil, K., Galceran, J., Tontsch, S., Roth, W. and Grosschedl, R. (2002) FGF4, a direct target of LEF1 and Wnt signaling, can rescue the arrest of tooth organogenesis in Lef1(−/−) mice. Genes Dev 16:3173–3185.

Lesot, H., Lisi, S., Peterkova, R., Peterka, M., Mitolo, V. and Ruch, J.V. (2001) Epigenetic signals during odontoblast differentiation. Adv Dent Res 15:8–13.

Linde, A. and Goldberg, M. (1993) Dentinogenesis. Crit Rev Oral Biol Med 4:679–728.

Miletich, I. and Sharpe, P.T. (2003) Normal and abnormal dental development. Hum Mol Genet 12(Spec No 1): R69–R73.

Nakashima, M., Nagasawa, H., Yamada, Y. and Reddi, A.H. (1994) Regulatory role of transforming growth factor-beta, bone morphogenetic protein-2, and protein-4 on gene expression of extracellular matrix proteins and differentiation of dental pulp cells. Dev Biol 162:18–28.

Nusse, R. (2003) Wnts and Hedgehogs: lipid-modified proteins and similarities in signaling mechanisms at the cell surface. Development 130:5297–5305.

Nybakken, K. and Perrimon, N. (2002) Heparan sulfate proteoglycan modulation of developmental signaling in Drosophila. Biochim Biophys Acta 1573:280–291.

Qin, C., Brunn, J.C., Cadena, E., Ridall, A., Tsujigiwa, H., Nagatsuka, H., Nagai, N. and Butler, W.T. (2002) The expression of dentin sialophosphoprotein gene in bone. J Dent Res 81:392–394.

Rajpar, M.H., Koch, M.J., Davies, R.M., Mellody, K.T., Kielty, C.M. and Dixon, M.J. (2002) Mutation of the signal peptide region of the bicistronic gene DSPP affects translocation to the endoplasmic reticulum and results in defective dentine biomineralization. Hum Mol Genet 11:2559–2565.

Ruch, J.V., Lesot, H., Karcher-Djuricic, V., Meyer, J.M. and Olive, M. (1982) Facts and hypotheses concerning the control of odontoblast differentiation. Differentiation 21:7–12.

Sarkar, L. and Sharpe, P.T. (1999) Expression of Wnt signalling pathway genes during tooth development. Mech Dev 85:197–200.

Shiba, H., Fujita, T., Doi, N., Nakamura, S., Nakanishi, K., Takemoto, T., Hino, T., Noshiro, M., Kawamoto, T., Kurihara, H. and Kato, Y. (1998) Differential effects of various growth factors and cytokines on the syntheses of DNA, type I collagen, laminin, fibronectin, osteonectin/secreted protein, acidic and rich in cysteine (SPARC), and alkaline phosphatase by human pulp cells in culture. J Cell Physiol 174:194–205.

Shields, E.D., Bixler, D. and el-Kafrawy, A.M. (1973) A proposed classification for heritable human dentine defects with a description of a new entity. Arch Oral Biol 18:543–553.

Sreenath, T., Thyagarajan, T., Hall, B., Longenecker, G., D'Souza, R., Hong, S., Wright, J.T., MacDougall, M., Sauk, J. and

Kulkarni, A.B. (2003) Dentin sialophosphoprotein knockout mouse teeth display widened predentin zone and develop defective dentin mineralization similar to human dentinogenesis imperfecta type III. J Biol Chem 278:24874–24880.

Taylor, S.M. and Jones, P.A. (1979) Multiple new phenotypes induced in 10T1/2 and 3T3 cells treated with 5-azacytidine. Cell 17:771–779.

Thesleff, I. and Aberg, T. (1999) Molecular regulation of tooth development. Bone 25:123–125.

Thesleff, I. and Hurmerinta, K. (1981) Tissue interactions in tooth development. Differentiation 18:75–88.

Thesleff, I. and Pratt, R.M. (1980) Tunicamycin inhibits mouse tooth morphogenesis and odontoblast differentiation in vitro. J Embryol Exp Morphol 58:195–208.

Thesleff, I., Keranen, S. and Jernvall, J. (2001) Enamel knots as signaling centers linking tooth morphogenesis and odontoblast differentiation. Adv Dent Res 15:14–18.

Thesleff, I., Partanen, A.M. and Vainio, S. (1991) Epithelial–mesenchymal interactions in tooth morphogenesis: the roles of extracellular matrix, growth factors, and cell surface receptors. J Craniofac Genet Dev Biol 11:229–237.

Thesleff, I., Vainio, S. and Jalkanen, M. (1989) Cell–matrix interactions in tooth development. Int J Dev Biol 33:91–97.

Tsukamoto, Y., Fukutani, S., Shin-Ike, T., Kubota, T., Sato, S., Suzuki, Y. and Mori, M. (1992) Mineralized nodule formation by cultures of human dental pulp-derived fibroblasts. Arch Oral Biol 37:1045–1055.

Vaahtokari, A., Aberg, T., Jernvall, J., Keranen, S. and Thesleff, I. (1996) The enamel knot as a signaling center in the developing mouse tooth. Mech Dev 54:39–43.

Vainio, S., Jalkanen, M. and Thesleff, I. (1989) Syndecan and tenascin expression is induced by epithelial–mesenchymal interactions in embryonic tooth mesenchyme. J Cell Biol 108: 1945–1953.

Vainio, S., Karavanova, I., Jowett, A. and Thesleff, I. (1993) Identification of BMP-4 as a signal mediating secondary induction between epithelial and mesenchymal tissues during early tooth development. Cell 75:45–58.

van Genderen, C., Okamura, R.M., Farinas, I., Quo, R.G., Parslow, T.G., Bruhn, L. and Grosschedl, R. (1994) Development of several organs that require inductive epithelial–mesenchymal interactions is impaired in LEF-1-deficient mice. Genes Dev 8:2691–2703.

Wang, J. and Shackleford, G.M. (1996) Murine Wnt10a and Wnt10b: cloning and expression in developing limbs, face and skin of embryos and in adults. Oncogene 13:1537–1544.

Xiao, S., Yu, C., Chou, X., Yuan, W., Wang, Y., Bu, L., Fu, G., Qian, M., Yang, J., Shi, Y., Hu, L., Han, B., Wang, Z., Huang, W., Liu, J., Chen, Z., Zhao, G. and Kong, X. (2001) Dentinogenesis imperfecta 1 with or without progressive hearing loss is associated with distinct mutations in DSPP. Nat Genet 27: 201–204.

Yamashiro, T., Tummers, M. and Thesleff, I. (2003) Expression of bone morphogenetic proteins and Msx genes during root formation. J Dent Res 82:172–176.

Yamazaki, H., Kunisada, T., Miyamoto, A., Tagaya, H. and Hayashi, S. (1999) Tooth-specific expression conferred by the regulatory sequences of rat dentin sialoprotein gene in transgenic mice. Biochem Biophys Res Commun 260:433–440.

Yuasa, K., Fukumoto, S., Kamasaki, Y., Yamada, A., Fukumoto, E., Kanaoka, K., Saito, K., Harada, H., Arikawa-Hirasawa, E., Miyagoe-Suzuki, Y., Takeda, S., Okamoto, K., Kato, Y. and Fujiwara, T. (2004) Laminin alpha2 is essential for odontoblast differentiation regulating dentin sialoprotein expression. J Biol Chem 279:10286–10292.

Zhang, X., Zhao, J., Li, C., Gao, S., Qiu, C., Liu, P., Wu, G., Qiang, B., Lo, W.H. and Shen, Y. (2001) DSPP mutation in dentinogenesis imperfecta Shields type II. Nat Genet 27:151–152.

Supplemental Material can be found at:
http://www.jbc.org/cgi/content/full/M611181200/DC1

THE JOURNAL OF BIOLOGICAL CHEMISTRY VOL. 282, NO. 32, pp. 23070–23080, August 10, 2007
© 2007 by The American Society for Biochemistry and Molecular Biology, Inc. Printed in the U.S.A.

PLAP-1/Asporin, a Novel Negative Regulator of Periodontal Ligament Mineralization*[S]

Received for publication, December 6, 2006, and in revised form, May 7, 2007 Published, JBC Papers in Press, May 23, 2007, DOI 10.1074/jbc.M611181200

Satoru Yamada[‡], Miki Tomoeda[‡], Yasuhiro Ozawa[‡], Shinya Yoneda[‡], Yoshimitsu Terashima[‡], Kazuhiko Ikezawa[‡], Shiro Ikegawa[§], Masahiro Saito[¶], Satoru Toyosawa[‖], and Shinya Murakami[‡1]

From the Departments of [‡]Periodontology and [‖]Oral Pathology, Osaka University Graduate School of Dentistry, Suita, Osaka 565-0871, Japan, [§]Laboratory for Bone and Joint Disease, Single Nucleotide Polymorphisms Research Center, The Institute of Physical and Chemical Research (RIKEN), Minato-ku, Tokyo 108-8639, Japan, and [¶]Department of Oral Medicine, Division of Operative Dentistry and Endodontics, Kanagawa Dental College, Yokosuka 238-8580, Japan

Periodontal ligament-associated protein-1 (PLAP-1)/asporin is a recently identified novel member of the small leucine-rich repeat proteoglycan family. PLAP-1/asporin is involved in chondrogenesis, and its involvement in the pathogenesis of osteoarthritis has been suggested. We report that *PLAP-1/asporin* is also expressed specifically and predominantly in the periodontal ligament (PDL) and that it negatively regulates the mineralization of PDL cells. *In situ* hybridization analysis revealed that *PLAP-1/asporin* was expressed specifically not only in the PDL of an erupted tooth but also in the dental follicle, which is the progenitor tissue of the PDL during tooth development. Overexpression of PLAP-1/asporin in mouse PDL-derived clone cells interfered with both naturally and bone morphogenetic protein 2 (BMP-2)-induced mineralization of the PDL cells. On the other hand, knockdown of *PLAP-1/asporin* transcript levels by RNA interference enhanced BMP-2-induced differentiation of PDL cells. Furthermore co-immunoprecipitation assays showed a direct interaction between PLAP-1/asporin and BMP-2 *in vitro*, and immunohistochemistry staining revealed the co-localization of PLAP-1/asporin and BMP-2 at the cellular level. These results suggest that PLAP-1/asporin plays a specific role(s) in the periodontal ligament as a negative regulator of cytodifferentiation and mineralization probably by regulating BMP-2 activity to prevent the periodontal ligament from developing non-physiological mineralization such as ankylosis.

Periodontal ligament (PDL)[2] tissue is a connective tissue that is interposed between the roots of the teeth and the inner wall of the tooth-supporting bone (alveolar bone) socket. The collagenous fibers form a meshwork that stretches out between the cementum covering the root surface and the bone and is firmly anchored by Sharpey fibers. The periodontal ligament links the teeth to the alveolar bone proper, providing support, protection, and sensory input to the masticatory system (1). In addition, the PDL also contributes to tooth nutrition, homeostasis, and the repair of damaged periodontal tissue. PDL cells originate in part from the ectomesenchyme of the investing layer of the dental follicle; this developmental origin gives these cells differential properties. Recently it has been revealed that PDL tissue possesses multipotential mesenchymal stem cells that can differentiate into mineralized tissue-forming cells such as osteoblasts and cementoblasts (2, 3). In fact, *in vitro* maintained PDL cells have various osteoblast-like properties, including the capacity to form mineralized nodules, expression of bone-associated markers, and response to bone-inductive factors such as bone morphogenetic protein 2 (BMP-2) (4, 5). Interestingly, however, PDL tissue is never ossified *in vivo* under normal circumstances. This suggests that some mechanisms exist to constitutively prevent unorchestrated osteogenesis and cementogenesis by PDL cells.

Previously we have reported the gene expression profile, described the quantitative aspects of the genes active in the human PDL, and identified a novel gene, *PLAP-1*, that is frequently expressed in human PDL tissue (6). An identical gene has been reported by other groups and named *asporin* because of its unique aspartic acid repeat at the N terminus of the mature protein (7, 8). The *PLAP-1/asporin* gene encodes a novel small leucine-rich repeat proteoglycan (SLRP) protein that resembles decorin and biglycan. Interestingly the expression of the *PLAP-1/asporin* gene was shown to be enhanced during the course of PDL cell cytodifferentiation into mineralized tissue-forming cells and is tightly regulated by BMP-2 (9).

Furthermore a recent report demonstrated that there is a significant association between a polymorphism in the aspartic acid repeat of the gene encoding PLAP-1/asporin and osteoarthritis, which is characterized by the progressive

* This work was supported by Grants-in-aid 17390560 and 17390561 from the Japan Society for the Promotion of Science and was a part of the 21st Century Center of Excellence entitled "Origination of Frontier BioDentistry" at Osaka University Graduate School of Dentistry supported by the Ministry of Education, Culture, Sports, Science and Technology. The costs of publication of this article were defrayed in part by the payment of page charges. This article must therefore be hereby marked "*advertisement*" in accordance with 18 U.S.C. Section 1734 solely to indicate this fact.

[S] The on-line version of this article (available at http://www.jbc.org) contains supplemental Table 1.

[1] To whom correspondence should be addressed: Dept. of Periodontology, Osaka University Graduate School of Dentistry, 1-8 Yamadaoka, Suita, Osaka 565-0871, Japan. Tel.: 81-6-6879-2930; Fax: 81-6-6879-2934; E-mail: ipshinya@dent.osaka-u.ac.jp.

[2] The abbreviations used are: PDL, periodontal ligament; PLAP-1, periodontal ligament-associated protein-1; SLRP, small leucine-rich repeat proteoglycan; BMP, bone morphogenetic protein; TGF, transforming growth factor; RT, reverse transcription; MEM, minimum Eagle's medium; FCS, fetal calf serum; FGF, fibroblast growth factor; ALPase, alkaline phosphatase; shRNA, small hairpin RNA; PBS, phosphate-buffered saline; E, embryonic day; MPDL, murine periodontal ligament; LRR, leucine-rich repeat.

Downloaded from www.jbc.org at OSAKA UNIVERSITY on August 7, 2007

loss of articular cartilage (10–12). It has also been shown that PLAP-1/asporin functioned as a negative regulator of chondrogenesis *in vitro* by inhibiting TGF-β function (10). Both articular cartilage and the PDL are rich in extracellular matrix and have a similar characteristic function, which involves cushioning the mechanical forces of the joints and teeth, respectively. These results suggest the possible involvement of PLAP-1/asporin in the regulation of PDL differentiation into hard tissue-forming cells.

To gain insight into PLAP-1/asporin functions in the PDL, we first examined the tissue distribution of *PLAP-1/asporin in vivo*. *In situ* hybridization analysis demonstrated specific and dominant expression of *PLAP-1/asporin* mRNA in the PDL. Furthermore during tooth development, strong mRNA expression of *PLAP-1/asporin* was observed in the dental follicle, which is the progenitor tissue that forms cementum, alveolar bone, and the PDL. We then examined an *in vitro* model of PDL differentiation that uses a PDL cell clone derived from mouse PDL tissues. Interestingly overexpression of PLAP-1/asporin in PDL cells repressed PDL differentiation and mineralization probably through BMP-2 signaling pathways. Conversely small interference RNA knockdown of *PLAP-1/asporin* in PDL cells augmented PDL differentiation induced by BMP-2. Furthermore co-immunoprecipitation experiments revealed that PLAP-1/asporin could bind to BMP-2 *in vitro*, and two-color immunohistochemistry staining showed co-localization of PLAP-1/asporin and BMP-2 at the cellular level. These data showed that *PLAP-1/asporin* is a periodontal ligament-specific gene that negatively regulates PDL differentiation and mineralization to ensure that the periodontal ligament is not ossified and to maintain homeostasis of the tooth-supporting system.

MATERIALS AND METHODS

RT-PCR Analysis—Total RNA was isolated from mouse tissues and cells using the QIA RNA isolation kit (Qiagen, Santa Clarita, CA) and then purified using the RNAeasy kit (Qiagen). Purified total RNA was reverse transcribed with SuperScript II reverse transcriptase (Invitrogen) with oligo(dT) primer. All PCRs were carried out using AmpliTaq Gold DNA polymerase (Roche Applied Science). The primers used in this study are listed in supplemental Table 1.

Probe Preparation—We subcloned the 709-bp 5′-end/EcoRI fragment, including the 5′-untranslated region and a portion of the open reading frame of mouse *PLAP-1/asporin* gene, into the pGEM-T easy vector (Promega, Madison, WI). The plasmid containing the *PLAP-1/asporin* insert was linearized by digestion with NcoI and SalI restriction enzymes to generate antisense and sense strands, respectively. In the presence of digoxigenin-labeled 11-dUTP (Roche Applied Science), the antisense and sense cRNA probes were prepared by *in vitro* transcription using SP6 and T7 RNA polymerases, respectively.

Northern Blot Analysis—Total RNA (15 μg) isolated from the maxillary and tibial tissues of 4-week-old BALB/c mice was electrophoresed on a 1% formaldehyde-agarose gel and transferred to a nitrocellulose filter (Roche Applied Science). The membranes were then hybridized overnight at 68 °C with digoxigenin-dUTP-labeled antisense single-stranded RNA probes specific for *PLAP-1/asporin* as described above. The blot was washed under high stringency (2× SSC, 0.1% SDS at room temperature) and low stringency (0.1× SSC, 0.1% SDS at 68 °C) conditions. The reaction was then blocked using the DIG (digoxigenin) Wash and Block Buffer Set (Roche Applied Science) according to the manufacturer's protocol. The hybrids were detected using the anti-digoxigenin-alkaline phosphatase Fab fragment (Roche Applied Science).

Tissue Preparation and in Situ Hybridization—To analyze erupted teeth, 4-week-old BALB/c mice were anesthetized by intraperitoneal injection of Nembutal (50 mg/kg of body weight) and intracardially perfused with physiological saline containing 5 units/ml heparin (Aventis Pharma, Tokyo, Japan) for 2–3 min followed by perfusion with 5% paraformaldehyde in 0.1 M sodium phosphate buffer (pH 7.4) at 4 °C for 15 min. The upper jaw samples containing the teeth were excised, and most of the soft tissue was removed. All of the samples were further fixed by immersion in the fixative described above overnight at 4 °C and then demineralized in buffered 10% EDTA at 4 °C under agitation for 7 days. The EDTA solution was changed daily. After processing, the blocks were rinsed and embedded in paraffin. Serial 5-μm-thick sections were cut in the transverse direction for the first molars and mounted onto aminopropylsilane-coated slides. Representative sections from each block were stained with hematoxylin and eosin. *In situ* hybridization of developing tooth germ was carried out on the fresh frozen horizontal sections of BALB/c mice fetal heads. The sections were fixed in 4% paraformaldehyde for 10 min, and this was followed by acetylation.

In situ hybridization was performed as described previously (13). We used the cRNA probe of *PLAP-1/asporin* described above. The sections were deparaffinized in xylene, hydrated, postfixed in 4% paraformaldehyde, and sequentially treated with 10 mg/ml proteinase K at 37 °C for 30 min and with 0.1 M triethanolamine containing 0.25% acetic anhydride for 10 min. Hybridization was done at 50 °C under high stringency conditions using the denatured probes at concentrations of about 1 ng/ml in a freshly prepared hybridization mixture. All samples were hybridized overnight at 50 °C. Posthybridization treatment included incubation with RNase A at 37 °C for 30 min followed by thorough washes. The washed slides were incubated with anti-digoxigenin monoclonal antibody (Roche Applied Science) overnight at 4 °C. After the application of biotinylated rabbit anti-mouse IgG antibody (Dako, Glostrup, Denmark), the sections were incubated with alkaline phosphatase-conjugated streptavidin (Dako) and then with nitro blue tetrazolium/5-bromo-4-chloro-3-indolyl phosphate solution (Roche Applied Science) for 3–5 h to visualize the hybridized sites. The activity of endogenous bone alkaline phosphatases in these specimens was inhibited by heating during paraffin embedding at 60 °C for 6 h. Negative controls for *in situ* hybridization were obtained by substituting the antisense probe with its sense probe.

Downloaded from www.jbc.org at OSAKA UNIVERSITY on August 7, 2007

Cloning of Mouse PDL Cell Line—Mouse PDL cells were obtained from the PDL tissues of the molar teeth obtained from 2.5-week-old BALB/c mice. The PDL tissues were scraped from the middle of one-third of the root surface and transferred into 24-well plates. The outgrown cells from the explants were cultured in α-MEM supplemented with 10% FCS, 10 ng/ml FGF-2 (Kaken, Kyoto, Japan), and 60 μg/ml kanamycin (Meijiseika, Tokyo, Japan). The cultures were maintained at 37 °C in a humidified atmosphere of 95% air and 5% CO_2. At subconfluence, the cells were passaged with trypsin-EDTA and cultured on tissue culture plates. After 12 subcultures, the cell suspension was diluted and plated on 96-well plates at a ratio of one or two cells per well. Cell cloning was done twice using the limiting dilution method in α-MEM supplemented with 10% FCS and 100 ng/ml FGF-2. Twenty-nine clonal cell lines were obtained and classified by alkaline phosphatase (ALPase) activity. One clonal cell line possessing the highest ALPase activity was selected and named MPDL22. The preosteoblastic cell line MC3T3-E1 was a generous gift from Prof. Toshiyuki Yoneda (Osaka University, Osaka, Japan).

Plasmids—We cloned the open reading frame of mouse *PLAP-1/asporin* gene into pCl-neo (Promega). We confirmed whole sequences of the insert by DNA sequencing and named it pCl-neo-PLAP-1/asporin. We used the pCl-neo plasmid vector without the insert as a negative control. We also cloned the open reading frame of mouse *PLAP-1/asporin* into p3XFLAG-CMV-14 (Sigma) in which the 3XFLAG protein can be fused to the C terminus of the insert. We named it p3XFLAG-PLAP-1/asporin. We used the p3XFLAG-CMV-14 vector without the insert as a negative control.

Cell Culture and Transfection—We maintained the MPDL22 cells in a standard medium of α-MEM supplemented with both 10% FCS and 100 ng/ml FGF-2. For stable transfections, we plated 5×10^4 of the MPDL22 cells/well in a 6-well plate. After 12 h, we transfected the cells with the pCl-neo-PLAP-1/asporin expression vector or the p3XFLAG-PLAP-1/asporin expression vector using Effectene transfection reagent (Invitrogen) in accordance with the manufacturer's protocol. After 24 h, we added G418 (400 μg/ml) to the culture medium to initiate drug selection. After selection, we evaluated *PLAP-1/asporin* expression using RT-PCR. We then established the stable transfectants overexpressing PLAP-1/asporin.

To differentiate transfected MPDL22 cells into hard tissue-forming cells *in vitro*, we cultured cells in a 24-well plate until they reached confluence. At this point, we removed FGF-2 from the culture medium and replaced the standard medium with α-MEM supplemented with 10% FCS, 10 mM β-glycerophosphate, and 50 μg/ml ascorbic acid (mineralization medium). We replaced the mineralization medium every 3 days. During the culture of the transfectant cells, we always added 400 μg/ml G418 to the mineralization medium.

To examine the effects of PLAP-1/asporin on BMP-2-induced cytodifferentiation, transfectant cells were cultured in standard medium in a 24-well plate until they reached confluence. On the next day, the medium was replaced with FCS-free α-MEM. After serum deprivation for 24 h, the cells were stimulated with 100 ng/ml BMP-2 (R&D Systems, Minneapolis, MN) in FCS-free α-MEM. The stimulated cells were then harvested at 24, 48, and 72 h after stimulation to assess ALPase activity.

RNA Interference of PLAP-1/Asporin—The small interference RNA oligonucleotide against mouse *PLAP-1/asporin* was designed according to Reynolds *et al.* (14). The target sequences included 5′-CGA TGA TGA CGA CAA CTC T-3′ and 5′-CCT GCA ACA TTT CGT TGT G-3′, which are located at nucleotides 326–344 and 1260–1278 of the mouse *PLAP-1/asporin* gene (GenBank™ accession number NM_025711), respectively. The pSilencer RNA interference kit (Ambion, Austin, TX) was used for generating small hairpin RNA (shRNA). We used a negative control shRNA oligonucleotide from the Ambion kit that is unrelated to *PLAP-1/asporin*. Briefly a double-stranded DNA oligonucleotide containing the shRNA and BamHI and HindIII overhangs was cloned into the BamHI and HindIII sites of the pSilencer 2.1-U6 hygro vector (Ambion), an expression vector designed to express shRNAs using the U6 promoter. The constructs were verified by DNA sequencing. The shRNA vectors were introduced into MPDL22 cells by Nucleofection (Amaxa, Gaithersburg, MD) according to the manufacturer's protocol. We started drug selection by hygromycin (600 μg/ml) 24 h after transfection.

Alkaline Phosphatase Activity and Mineralization Assay—ALPase activity was assessed according to the procedure of Bessey *et al.* (15). Briefly after washing twice with PBS, the cells were homogenized in a glass homogenizer in 1 ml of 0.9% NaCl, 0.2% Triton X-100 at 4 °C and then centrifuged for 15 min at 12,000 × *g*. ALPase activity in the supernatant was measured using *p*-nitrophenyl phosphate as a substrate. Subsequently the supernatant was mixed with 0.5 M Tris-HCl buffer (pH 9.0) containing 0.5 mM *p*-nitrophenyl phosphate and 0.5 mM $MgCl_2$. Next the samples were incubated at 37 °C for 30 min, and the reaction was stopped by addition of 0.25 ml of 1 N NaOH. Using a spectrometer, hydrolysis of *p*-nitrophenyl phosphate was monitored as a change in A_{410}; *p*-nitrophenol was used as a standard. One unit of activity was defined as the enzyme activity hydrolyzing 1 nmol of *p*-nitrophenyl phosphate in 30 min. The histochemical method that was used for staining calcified nodules was done using the alizarin red staining method of Dahl (16). The cell layers were washed twice with PBS and then fixed in dehydrated ethanol. After fixation, the cell layers were stained with 1% alizarin red S in 0.1% NH_4OH (pH 6.3–6.5) for 5 min. The dishes were washed with H_2O and then observed microscopically.

Cellular DNA Contents—DNA content was measured using a modification of the method of Labarca and Paigen (17). The cells were washed with PBS and then homogenized at 4 °C in 1 ml of 2 M NaCl, 25 mM Tris-HCl (pH 7.4). After centrifugation at 12, 000 × *g* for 10 min, 25 μl of 5 μg/ml bisbenzimidazole (Hoechst 33258) were added to 100 μl of the supernatant. After excitation at 356 nm, the fluorescent spectra of the emission at 458 nm were monitored using a spectrophotometer (microplate reader MTP-32, Corona Electric, Ibaragi, Japan). The concentration of DNA in the samples was determined using a standard curve based on various concentrations of calf thymus DNA.

Downloaded from www.jbc.org at OSAKA UNIVERSITY on August 7, 2007

[^{3}H]Thymidine Incorporation Assay—The proliferation activity of the *PLAP-1/asporin* overexpressing transfectant cells and *PLAP-1/asporin* shRNA transfectant cells was assessed by measuring the [^{3}H]thymidine incorporation. The cells were seeded to 24-well culture dishes (1×10^4 cells/well). On the next day, the medium was replaced with FCS-free α-MEM. After serum deprivation for 24 h, the cells were stimulated with α-MEM containing 10% FCS for 24 h. DNA synthesis was measured by pulsing wells with 2 μCi/well [^{3}H]thymidine for 4 h. The cells were then washed three times with PBS, and soluble radioactivity was extracted with 5% trichloroacetic acid. The cells were solubilized in 1 N NaOH, and lysate was brought to a neutral pH by addition of 6 N HCl. The incorporated radioactivity was determined in a liquid scintillation counter (Aloka, Tokyo, Japan) using an aqueous scintillation mixture.

Expression and Purification of Recombinant PLAP-1/Asporin—Recombinant mouse PLAP-1/asporin protein was generated from baculovirus-infected silkworms as described previously (18). Briefly we subcloned the full length of mouse *PLAP-1/asporin* cDNA into the transfer vector pSYNGCH_Th that was to be fused to a His tag in the C terminus. Then the plasmid was co-transfected with the linearized baculovirus DNA BacDuo (Katakura Industries, Saitama, Japan) into the *Spodoptera frugipedra* cell line SF21AE. Three days after transfection, the culture supernatants containing the recombinant baculovirus were harvested. The recombinant virus was injected into the body cavities of silkworm larvae (8.0×10^5 plaque-forming units/head). The whole body of the infected larvae was mechanically blended in lysis buffer (20 mM Na_2PO_4, pH 7.5, 10% glycerol, 0.15 M NaCl, 1 mM phenylmethylsulfonyl fluoride, 10 mM benzamide, 1 mM dithiothreitol, 1 mM EGTA, 1 mM EDTA). Homogenized lysates were centrifuged at 80,000 × *g* for 60 min, and the supernatants were then diluted five times by dilution buffer (20 mM NaH_2PO_4, pH 8.0, 0.3% Zwittergent 3-14). The diluted solution was loaded on a nickel-Sepharose column. After washing with washing buffer (20 mM NaH_2PO_4, pH 8.0, 0.3% Zwittergent 3-14), His-tagged mouse PLAP-1/asporin was eluted by elution buffer (20 mM Tris-HCl, pH 8.0, 0.3 M NaCl, 250 mM imidazole, 10% glycerol, 0.1% Zwittergent 3-14, 0.05% 2-mercaptoethanol).

To confirm the quality of recombinant protein, the elution sample was subjected to SDS-PAGE (5–20% gradient gel). The proteins separated in the gel were stained using Silver Stain II kit (Wako, Osaka, Japan). After the SDS-PAGE, electroblotting onto polyvinylidene difluoride membranes was performed. The membranes were incubated in TBST (50 mM Tris-HCl, pH 7.5, 150 mM NaCl, 0.1% (v/v) Tween 20) with 5% (w/v) nonfat dried milk at 4 °C overnight, washed in TBST three times, and incubated with primary antibody in TBST containing 5% milk for 1 h at room temperature. The primary antibody was a rabbit polyclonal anti-polyhistidine antibody (Santa Cruz Biotechnology, Santa Cruz, CA) at 1:1,000. After further washing in TBST, membranes were incubated for 1 h with horseradish peroxidase-linked anti-rabbit IgG secondary antibody (Amersham Biosciences), and immunoreactive proteins were detected using the ECL kit (Amersham Biosciences).

Co-immunoprecipitation Assay and Western Blotting—Recombinant PLAP-1/asporin protein (1.2 μg) was incubated with 3.0 μg of BMP-2 for 1 h at 4 °C in 0.5 ml of binding buffer (50 mM Tris-HCl, pH 7.5, 150 mM NaCl, 1% Triton X-100, Complete protease inhibitor mixture (Roche Applied Science)). Then 7.5 μl of anti-polyhistidine antibody-conjugated agarose (Santa Cruz Biotechnology) or 40 μl of anti-BMP-2 antibody (Calbiochem-Novabiochem)-conjugated Protein G-Sepharose (Amersham Biosciences) were added to the reaction and incubated for 1 h at 4 °C. The precipitates were washed three times with binding buffer, subjected to 15% SDS-PAGE, and then electroblotted onto polyvinylidene difluoride membranes. The membranes were incubated in TBST with 5% (w/v) nonfat dried milk at 4 °C overnight, washed in TBST three times, and incubated with primary antibody in TBST containing 5% milk for 1 h at room temperature. The primary antibodies were a rabbit polyclonal anti-polyhistidine antibody at 1:1,000 and a goat polyclonal anti-BMP-2/4 antibody (R&D Systems) at 1:250. After further washing in TBST, membranes were incubated for 1 h with horseradish peroxidase-linked anti-rabbit IgG secondary antibody (Amersham Biosciences) or anti-goat IgG secondary antibody (Santa Cruz Biotechnology), and immunoreactive proteins were detected using the ECL kit.

Immunohistochemistry—The FLAG-tagged PLAP-1/asporin-transfected MPDL22 cells were seeded on a collagen type I-coated 10-mm glass-bottomed dish (Matsunami, Osaka, Japan). On the next day, to detect BMP-2 binding, the cells were preincubated with BMP-2 (10 μg/ml) for 2 h at 37 °C and washed with PBS three times. The cells were fixed in a mixture of methanol:acetone (1:1) for 1 min at room temperature, then washed with PBS three times, and preblocked in PBS containing 10% bovine serum albumin (Sigma) for 30 min at room temperature. The BMP-2-positive cells were identified by incubation with biotinylated anti-BMP-2/4 antibody (2.5 μg/ml, R&D Systems) overnight at 4 °C and subsequently streptavidin-rhodamine red (Invitrogen) for 1 h at room temperature. After washing with PBS, the cells were incubated with fluorescein isothiocyanate-conjugated anti-FLAG antibody (Sigma) for 1 h at room temperature. Then the cells were washed, and the nuclei were stained with 4′,6-diamidino-2-phenylindole (Vector Laboratories, Burlingame, CA).

Statistical Analysis—All of the experiments in this study were conducted at least three times. The data shown are representative results. Experimental values are given as means ± S.D. of triplicate assays. The statistical significance of the differences between two means was examined by the Mann-Whitney *U* test; *p* values less than 0.05 were considered to indicate a significant difference.

RESULTS

Specific Expression of PLAP-1/Asporin in the Periodontal Ligament—We analyzed *PLAP-1/asporin* expression in various mouse tissues. RT-PCR analysis revealed dominant expression of *PLAP-1/asporin* in the maxilla, which contains teeth and periodontal tissues consisting of gingiva, cementum, alveolar bone, and the PDL (Fig. 1*A*). Our previous study showed dom-

Downloaded from www.jbc.org at OSAKA UNIVERSITY on August 7, 2007

inant expression of *PLAP-1/asporin* in human PDL tissue (6). On the other hand, *PLAP-1/asporin* mRNA has been shown to be expressed abundantly in the heart in both mice and humans (7, 8). However, as Fig. 1*A* indicates, the maxilla, which contains PDL tissues, had a higher expression of *PLAP-1/asporin* mRNA than the heart (Fig. 1*A*). These results prompted us to investigate the specific expression of *PLAP-1/asporin* in periodontal tissues.

Next we performed Northern blot analysis to assess the *in vivo* expression of *PLAP-1/asporin* mRNA in the maxilla, which includes both teeth and periodontal tissues. We selected the 5′-region of *PLAP-1/asporin* mRNA, which has nucleotide sequences specific to *PLAP-1/asporin*, to use as a probe. The analysis revealed specific detection of the 2.3-kb transcript of *PLAP-1/asporin* in the maxilla (Fig. 1*B*). Notably there was no *PLAP-1/asporin* signal in the bone tissue obtained from the tibia, suggesting that *PLAP-1/asporin* is not expressed in the bone compartment of the maxilla.

We then carried out an *in situ* hybridization analysis of *PLAP-1/asporin* expression in mouse maxilla specimens. *PLAP-1/asporin* was expressed only in PDL tissue (Fig. 2*A*).

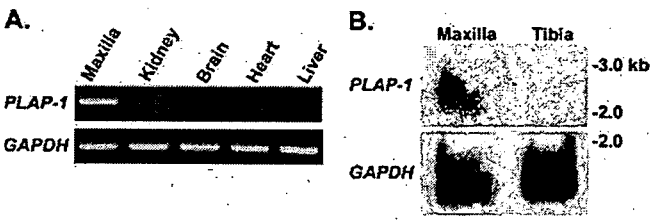

FIGURE 1. **Tissue distribution of *PLAP-1/asporin* mRNA.** *A*, RT-PCR analysis in various tissues from 4-week-old BALB/c mice. The number of PCR cycles was 28 and 22 for *PLAP-1/asporin* and glyceraldehyde-3-phosphate dehydrogenase (*GAPDH*), respectively. *B*, Northern blot analysis in the maxilla and tibia. Total RNA (15 μg) from the maxilla and tibia was electrophoresed.

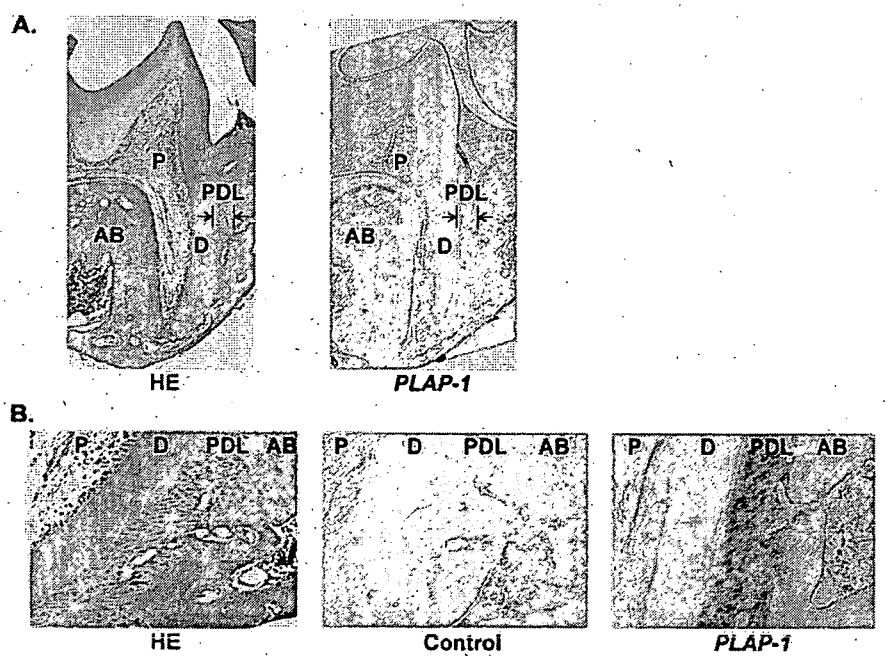

FIGURE 2. **Specific expression of *PLAP-1/asporin* in the periodontal ligament *in vivo*.** *A*, *in situ* hybridization analysis in the mouse maxilla from 4-week-old BALB/c mice. *B*, higher magnification. *HE*, hematoxylin and eosin stain; *PLAP-1*, antisense probe for *PLAP-1/asporin*; *Control*, sense probe for *PLAP-1/asporin*; *P*, pulp; *D*, dentin; *AB*, alveolar bone. *Original magnification*, ×50 in *A* and ×200 in *B*.

High magnification showed broad and intense expression of *PLAP-1/asporin* mRNA in the PDL tissue (Fig. 2*B*). No expression was observed in alveolar bone or other periodontal tissues such as gingival tissue, the bone marrow of alveolar bone, or dental pulp tissue. This suggests that PLAP-1/asporin presumably plays a particular *in vivo* role in the periodontal ligament tissue.

PLAP-1/Asporin Expression during Tooth Development—To obtain a more complete picture of *in vivo PLAP-1/asporin* expression in the periodontal ligament, particularly during tooth development, we performed an *in situ* hybridization analysis of tooth germs at different stages of development. As shown in Fig. 3*A*, around embryonic day 13 (E13), the dental epithelium invaginates into the neural crest-derived dental ectomesenchyme and forms the epithelial bud, which is known as the bud stage. Subsequently during the following cap stage around E15.5, the dental epithelium starts to differentiate into inner and outer dental epithelia. During the early bell stage around E18, specific cusp pattern formation commences. During the late bell stage, which occurs around postnatal day 1, dentin matrix is secreted at the tip of the cusps by functional odontoblasts, and terminal differentiation of ameloblasts begins.

No expression of *PLAP-1/asporin* mRNA was observed in the tooth germ at the bud stage at E13 (Fig. 3*B*). Then at the cap stage, strong expression was detected only in the dental follicle, which originates from the neural crest-derived ectomesenchyme (Fig. 3*C*). The dental follicle gives rise to the periodontal tissues consisting of periodontal ligament, cementum, and alveolar bone. *PLAP-1/asporin* mRNA was expressed neither in the dental papilla, which forms the dentin and pulp, nor in the dental epithelium. During the bell stage, continuous expression of *PLAP-1/asporin* was observed in dental follicles, especially in those in which tooth root formation was taking place (Fig. 3, *D* and *E*). Taken together, the data indicate that *PLAP-1/asporin* is initially expressed in the dental follicle cells during tooth germ development, and specific expression of *PLAP-1/asporin* becomes progressively evident in adult PDL tissue.

Establishment of the Mouse Periodontal Ligament Cell Line MPDL22—To analyze PLAP-1/asporin function *in vitro*, we established PDL cell clones from mouse PDL tissue. Utilizing the dilution cloning method in the presence of FGF-2, we obtained 29 cell clones from explant cultures of mouse PDL tissue. To assess their ability for cytodifferentiation into hard tissue-forming cells, we cultured each cell clone in the mineralization medium for 8 days (Fig. 4).

Downloaded from www.jbc.org at OSAKA UNIVERSITY on August 7, 2007

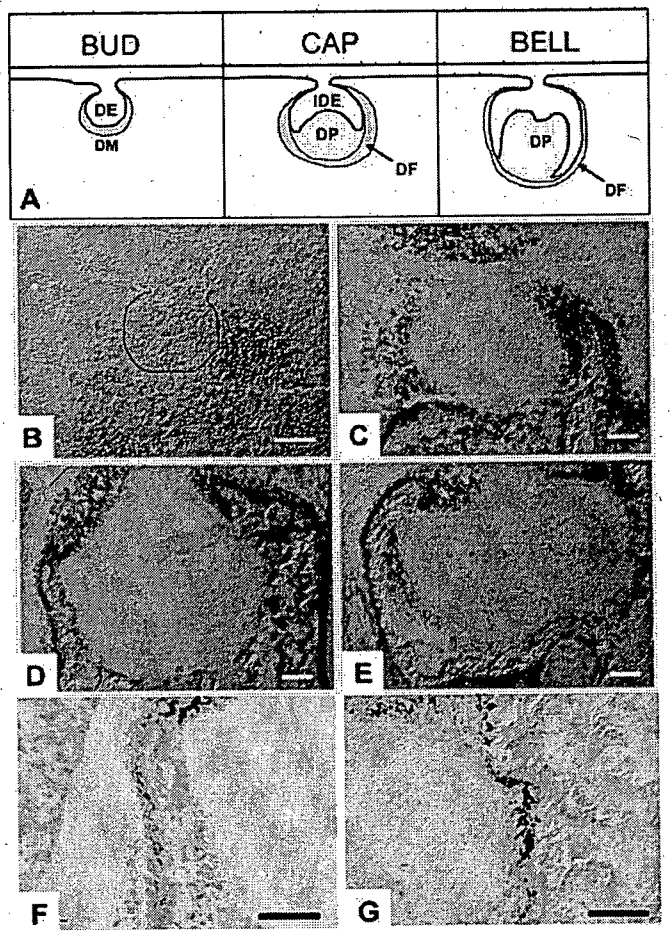

FIGURE 3. ***PLAP-1/asporin* expression in tooth development.** *A*, schematic representation of molar tooth development. *DE*, dental epithelium; *DM*, dental mesenchyme; *IDE*, inner enamel epithelium; *DP*, dental papilla; *DF*, dental follicle. *B–G*, *in situ* hybridization of *PLAP-1/asporin* in tooth germ at different stages of development. *B*, no expression at the bud stage (E13). The *black line* shows an outline of the tooth germ. *C*, restricted expression to the dental follicle at the cap stage (E15.5). *D*, early bell stage (E18). *E*, late bell stage (postnatal day 1). There is continuous expression of *PLAP-1/asporin* in dental follicle throughout the early and late bell stages. *F*, higher magnification of *D*. *G*, higher magnification of *E*. *Scale bars*, 100 μm.

Among the cell lines, one cell line, designated MPDL22, showed the highest ALPase activity and formed calcified nodules during culture. Thus, we selected MPDL22 for further characterization.

We assessed the expression of mineralized tissue-related genes in MPDL22 (Fig. 5). We cultured various cell clones in the mineralization medium for 8 days and then performed RT-PCR analysis. MPDL22 cells were positive for various extracellular matrix genes, collagen type I, collagen type III, collagen type XII, periostin, *PLAP-1/asporin*, and osteopontin (Fig. 5*B*). In terms of osteoblastic transcriptional factors, MPDL22 cells were positive for *Runx2*, *Msx2*, *Dlx5*, and Osterix (Fig. 5*A*). MG/B6 cells, derived from mouse gingival connective tissues, were also cultured in the mineralization medium. As expected, MG/B6 showed no ALPase activity even when the cells were cultured in the mineralization medium. Moreover MG/B6 demonstrated no expression of osteoblastic transcriptional factors and collagen type XII, periostin, and *PLAP-1/asporin*. We concluded that MPDL22 had a high potential for mineralization and could be a progenitor of osteoblasts or cementoblasts. In this study, we used MPDL22 as host cells for further investigation.

Overexpression of PLAP-1/Asporin in MPDL22 Suppresses Cytodifferentiation and Mineralization—To explore the role of PLAP-1/asporin in PDL cell cytodifferentiation and mineralization, we established MPDL22 cells overexpressing PLAP-1/asporin. We transfected the MPDL22 cells with the vector expressing PLAP-1/asporin. After drug selection, we established stable transfectants that were overexpressing PLAP-1/asporin (Fig. 6*A*). We cultured the transfected cells in mineralization medium and measured ALPase activity (Fig. 6*B*). ALPase activity of the transfectants overexpressing PLAP-1/asporin was significantly suppressed during culture compared with the ALPase activity of mock-transfected control MPDL22 cells (Fig. 6*B*). Alizarin red S staining of the transfectants on days 12 and 15 of culture revealed that calcified nodule formation of the transfectant overexpressing PLAP-1/asporin was suppressed compared with that of mock-transfected control MPDL22 cells (Fig. 6*C*). These results suggest that PLAP-1/asporin may negatively regulate PDL cell mineralization.

PLAP-1/Asporin Regulates BMP-2-induced Cytodifferentiation of MPDL22—BMP-2 is one of the most potent cytokines that stimulates osteoblast differentiation and bone formation (19). BMP-2 has also been reported to stimulate osteoblastic differentiation of human PDL cells (20) and to promote dental follicle cells that are putative progenitor cells for the periodontium that differentiate into a cementoblastic/osteoblastic phenotype (21). As expected, BMP-2 enhanced the ALPase activity and the calcified nodule

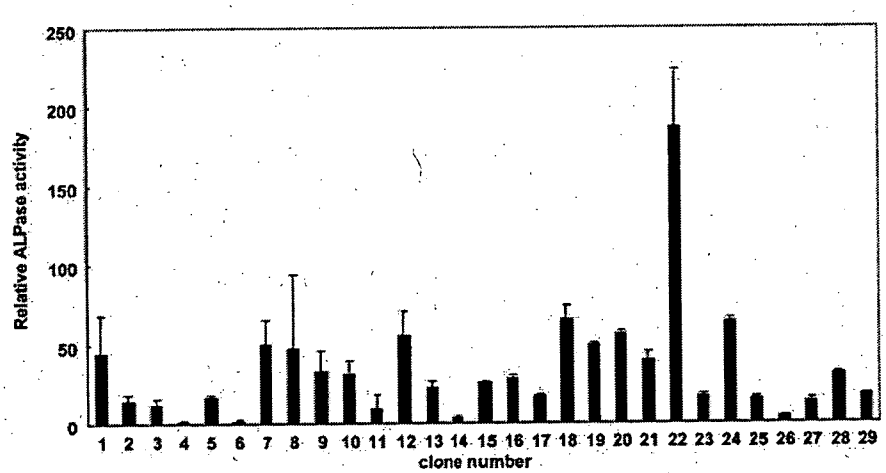

FIGURE 4. **ALPase activities of mouse PDL cell clones after 8 days in the mineralization medium.** Results are presented as the ratio of ALPase activity of each clone to clone number 4 (MPDL4). Clone number 22 (MPDL22) showed the highest ALPase activity. The values are given as means ± S.D. of triplicate assays. For reference, the ratio of ALPase activity of MG/B6 (see Fig. 5), which was derived from mouse gingival connective tissues, was 0.18 ± 0.34.

Downloaded from www.jbc.org at OSAKA UNIVERSITY on August 7, 2007

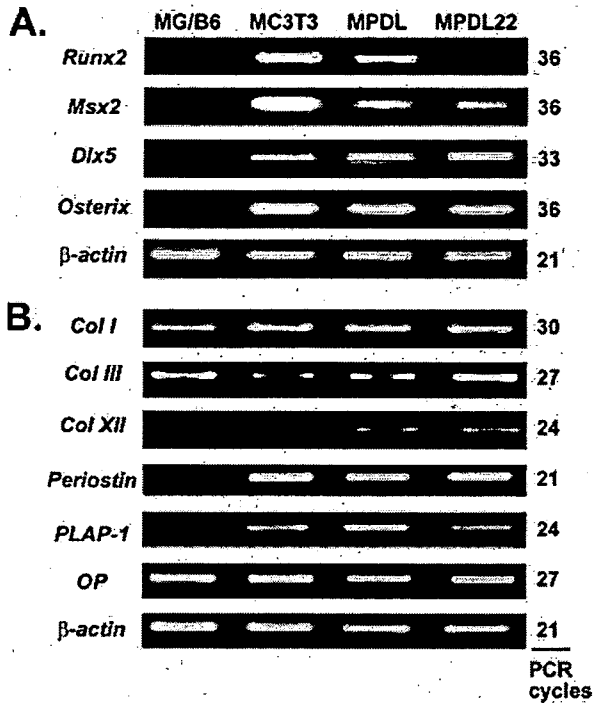

FIGURE 5. **RT-PCR analysis of genes related to mineralized tissue in MPDL22.** *A*, transcriptional factors. MPDL22 showed positive expression of *Runx2*, *Msx2*, *Dlx5*, and Osterix, which are osteoblastic transcriptional factors. MG/B6, a mouse gingival fibroblast cell clone, showed no expression of osteoblastic transcriptional factors. *B*, extracellular matrix genes. MPDL22 expressed all of the extracellular matrix transcripts that were analyzed. MC3T3-E1 showed weak expression of collagen (*Col*) type III and type XII. *OP*, osteopontin.

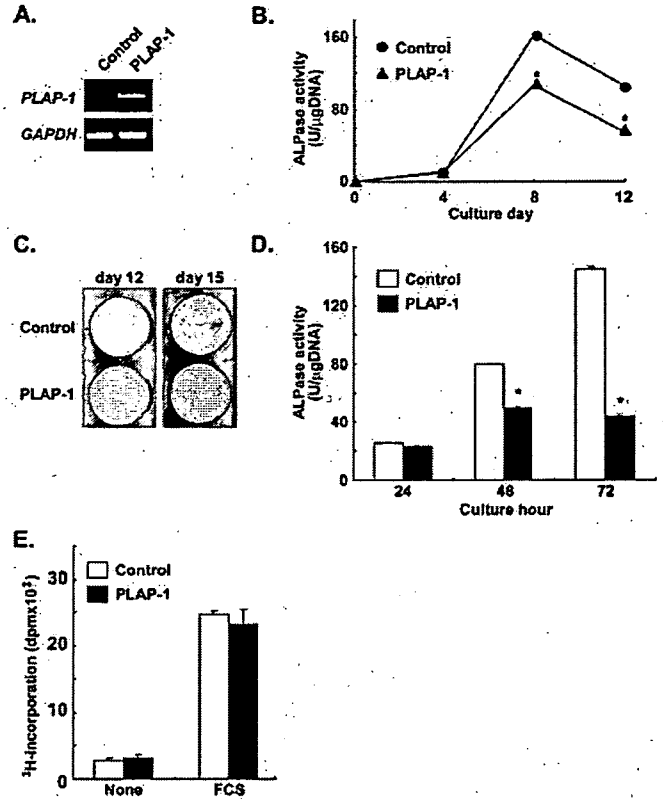

FIGURE 6. **Overexpression of PLAP-1/asporin in MPDL22 suppresses cytodifferentiation and mineralization.** *A*, RT-PCR analysis of *PLAP-1/asporin* expression in the transfected MPDL22 cells. *B*, PLAP-1/asporin inhibits ALPase activities. The values are given as means ± S.D. of triplicate assays. *, $p < 0.05$. *C*, PLAP-1/asporin suppresses calcified nodule formation. Alizarin red staining was performed after culture in mineralization medium for 12 and 15 days. *D*, PLAP-1/asporin inhibits BMP-2-induced ALPase activities. Shown are ALPase activities after stimulation by BMP-2 (100 ng/ml) for the indicated hours. The values are given as means ± S.D. of triplicate assays. *, $p < 0.05$. *E*, PLAP-1/asporin does not suppress proliferation activities. Shown is [^{3}H]thymidine incorporation of the transfected MPDL22 cells after stimulation by 10% FCS. The values are given as means ± S.D. of triplicate assays. Representative results of three independent experiments are shown. *GAPDH*, glyceraldehyde-3-phosphate dehydrogenase; *U*, units.

formation of MPDL22 cells (data not shown). On the other hand, in human PDL cells, *PLAP-1/asporin* transcript was regulated by BMP-2, and BMP-2 stimulation of human PDL cells up-regulated PLAP-1/asporin expression (9). Given that BMP-2 induced PDL cell cytodifferentiation and mineralization, we speculated that PLAP-1/asporin could negatively regulate PDL cell cytodifferentiation and mineralization through BMP-2. Thus, we examined the effects of overexpressing PLAP-1/asporin on BMP-2-induced MPDL cell cytodifferentiation (Fig. 6*D*). BMP-2 induced ALPase activity of the mock-transfected control MPDL22 cells. On the other hand, BMP-2-induced ALPase activity in the transfectants overexpressing PLAP-1/asporin was significantly inhibited. These results suggest that PLAP-1/asporin negatively regulates MPDL22 cell cytodifferentiation and mineralization through BMP-2 functions. Furthermore we assessed whether or not the effect of PLAP-1/asporin overexpression could be general suppression of cellular activities. We stimulated the transfectant cells with 10% FCS and assessed the proliferation activities (Fig. 6*E*). The transfectant cells overexpressing PLAP-1/asporin showed proliferation activity equivalent to the mock-transfected control cells by FCS stimulation. These results reveal that overexpression of PLAP-1/asporin does not result in general suppression of the cellular activity.

To examine the effects of PLAP-1/asporin knockdown on BMP-2-induced cytodifferentiation, we established MPDL transfectant cells that had shRNA introduced for the *PLAP-1/asporin* gene. We designed two different shRNA sequences specific for *PLAP-1/asporin* mRNA and constructed two independent shRNA expression plasmids. We obtained two different transfectant cell lines by stably transfecting the MPDL22 cells with each plasmid independently. These cell lines showed reduced *PLAP-1/asporin* transcript expression (Fig. 7*A*). One transfectant cell line, 326i, showed complete reduction of the *PLAP-1/asporin* transcript. On the other hand, 1260i showed a partial reduction of the transcript. To assess the effects of *PLAP-1/asporin* RNA interference on BMP-2-induced ALPase activity, we assayed the activity of ALPase on BMP-2 stimulation (Fig. 7*B*). 326i showed significant hyper-responsiveness to BMP-2 stimulation; 1260i also showed significant enhancement of ALPase activity. However, consistent with the reduced *PLAP-1/asporin* transcript level, the enhancement of ALPase activity in 1260i was lower than that in 326i. We then assayed BMP-2-induced gene expression by RT-PCR analysis (Fig. 7*C*). 326i and 1260i showed strong induction of BMP-2-induced bone sialoprotein and osteocalcin expression compared with con-

Downloaded from www.jbc.org at OSAKA UNIVERSITY on August 7, 2007

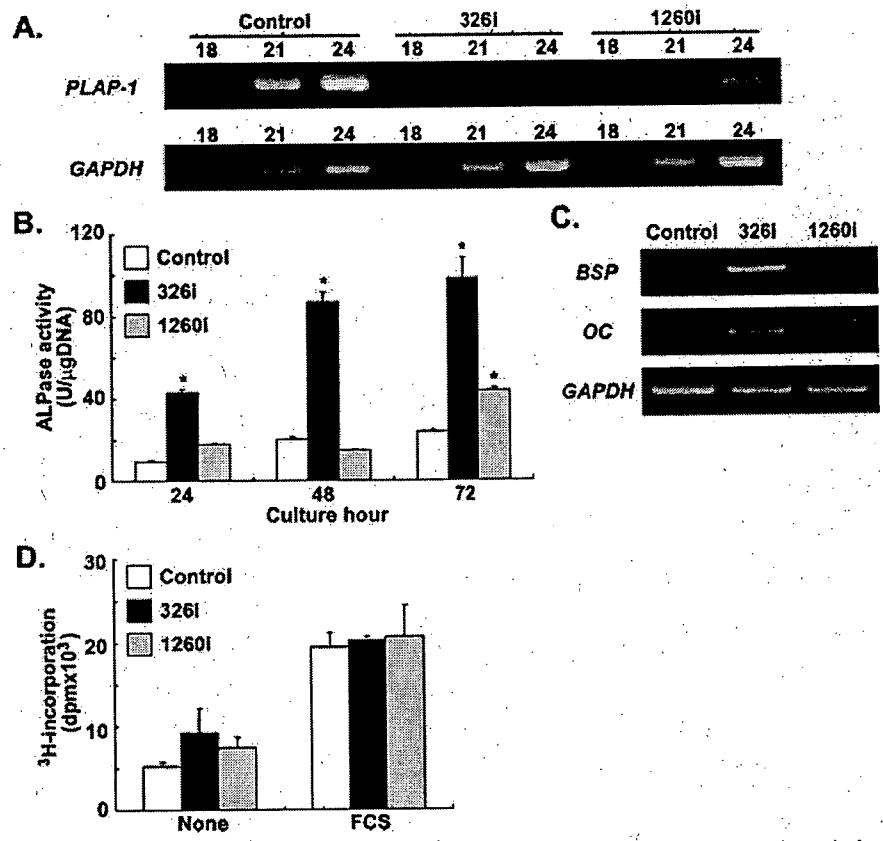

FIGURE 7. **Stable knockdown of *PLAP-1/asporin* increases BMP-2-induced cytodifferentiation of MPDL22.** *A*, steady-state levels of *PLAP-1/asporin* in MPDL22 cells. RT-PCR analysis of *PLAP-1/asporin* was carried out. The number of PCR cycles is shown *above* each *lane*. *Control*, MPDL22 stably transfected with an expression vector for control shRNA; *326i*, MPDL22 stably transfected with an expression vector for *PLAP-1/asporin* shRNA in target site 326; *1260i*, MPDL22 stably transfected with an expression vector for *PLAP-1/asporin* shRNA in target site 1260. *B*, increased response to BMP-2 following knockdown of *PLAP-1/asporin*. MPDL22 cells stably transfected with control or *PLAP-1/asporin* shRNA expression vector were treated with 100 ng/ml BMP-2. ALPase activities of the transfectants were assayed after BMP-2 stimulation for 24, 48, and 72 h. The values are given as means ± S.D. of triplicate assays. *, $p < 0.05$. *C*, strong induction of BMP-2-induced gene expression in *PLAP-1/asporin* shRNA transfectants. RT-PCR analysis was performed after BMP-2 stimulation for 48 h. The number of PCR cycles was 33, 30, and 22 for bone sialoprotein (*BSP*), osteocalcin (*OC*), and glyceraldehyde-3-phosphate dehydrogenase (*GAPDH*), respectively. *D*, RNA interference of *PLAP-1/asporin* does not suppress proliferation activities. Shown is [^{3}H]thymidine incorporation of the shRNA-transfected MPDL22 cells after stimulation by 10% FCS. The values are given as means ± S.D. of triplicate assays. Representative results of three independent experiments are shown. *U*, units.

trol cells. The enhancement of bone sialoprotein and osteocalcin gene expression in 1260i was also lower than that in 326i, consistent with the reduced *PLAP-1/asporin* transcript level. Then we assessed whether or not RNA interference of *PLAP-1/asporin* could affect the general cellular activity. We stimulated the shRNA transfectant cells with 10% FCS and assessed the proliferation activities (Fig. 7*D*). 326i and 1260i cells showed proliferation activity equivalent to the control cells by FCS stimulation. These results indicate that RNA interference of *PLAP-1/asporin* does not affect the general cellular activity.

PLAP-1/Asporin Binds to BMP-2 in Vitro—It has been reported that other SLRP family proteins (including decorin, biglycan, and PLAP-1/asporin) bind to TGF-β1 (10, 22). In addition, biglycan binds to BMP-4 (23). These observations suggest the possibility that PLAP-1/asporin can also interact with BMP-2. We investigated this possibility by testing the ability of recombinant PLAP-1/asporin protein to bind BMP-2 (Fig. 8). First we confirmed the purity of silkworm-derived recombinant His-tagged PLAP-1/asporin protein by SDS-PAGE and Western blot analysis using anti-His antibody (Fig. 8*A*). Recombinant PLAP-1/asporin protein was detected at around 43 kDa, which is the expected molecular mass of PLAP-1/asporin protein (7) by SDS-PAGE and Western blot analysis under the reduced condition. We then performed immunoprecipitation experiments using the recombinant His-tagged PLAP-1/asporin protein and BMP-2 (Fig. 8*B*). We found that PLAP-1/asporin co-precipitated with BMP-2 (Fig. 8*B*, *lane 2*). Reciprocal co-immunoprecipitation experiments also showed that PLAP-1/asporin can be found in the BMP-2 precipitate (Fig. 8*B*, *lane 4*). These results confirm the direct *in vitro* interaction between PLAP-1/asporin and BMP-2.

Co-localization of PLAP-1/Asporin and BMP-2 in MPDL22 Cells—To further understand the relationship between PLAP-1/asporin and BMP-2 binding at a cellular level, we performed two-color immunohistochemical staining of FLAG-tagged PLAP-1/asporin-transfected MPDL22 cells, which were preincubated with BMP-2 using anti-FLAG and anti-BMP-2 antibodies (Fig. 7). The co-localization of PLAP-1/asporin (*green*) and BMP-2 (*red*) were detected coincidentally in the FLAG-tagged PLAP-1/asporin-transfected MPDL22 cells, shown in the *orange* staining (Fig. 9*F*). This shows that PLAP-1/asporin and BMP-2 can bind at a cellular level. Interestingly the FLAG-tagged PLAP-1/asporin-transfected MPDL22 cells show more BMP-2 binding than mock-transfected control MPDL22 cells. This suggests that PLAP-1/asporin could control BMP-2 binding at the cellular level.

DISCUSSION

In this study, we have described the localization and potential function of PLAP-1/asporin. Our data demonstrate that *PLAP-1/asporin* is a PDL-specific gene that negatively regulates PDL cell cytodifferentiation and mineralization. The localization of PLAP-1/asporin is unique. The similar localization is not found with any other member of the small leucine-rich repeat proteoglycan family. We recently reported that the expression of PLAP-1/asporin is tightly regulated by BMP-2, one of the

Downloaded from www.jbc.org at OSAKA UNIVERSITY on August 7, 2007

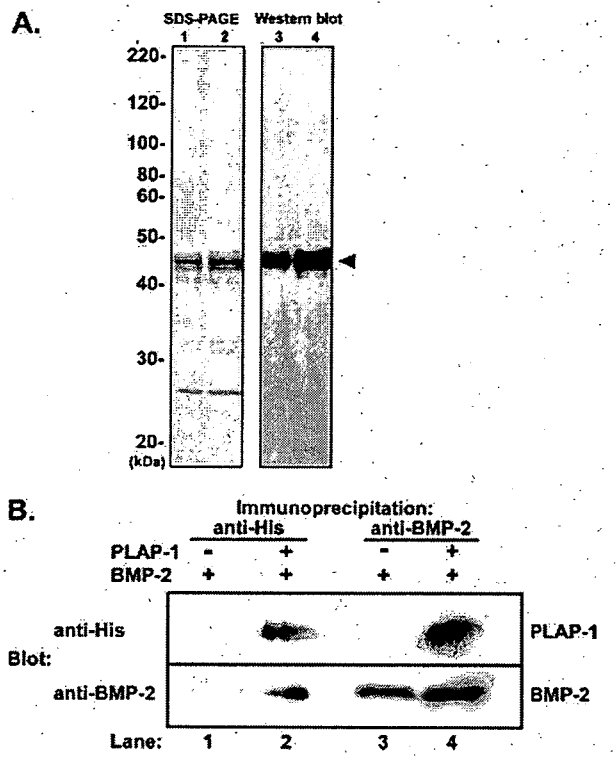

FIGURE 8. **PLAP-1/asporin binds to BMP-2 *in vitro*.** *A*, SDS-PAGE and Western blot analysis of the recombinant PLAP-1/asporin. Purified silkworm-derived His-tagged PLAP-1/asporin protein was analyzed by SDS-PAGE and Western blotting under reduced condition. The SDS-PAGE gel was stained with silver staining. His-tagged PLAP-1/asporin was detected with anti-polyhistidine antibody in Western blotting. *Lanes 1* and *3*, 0.3 μg of recombinant PLAP-1/asporin was applied. *Lane 2* and *4*, 0.6 μg of recombinant PLAP-1/asporin was applied. The *arrowhead* indicates recombinant PLAP-1/asporin protein. Positions of molecular mass markers are shown on the *left side*. *B*, recombinant BMP-2 was incubated with or without His-tagged PLAP-1/asporin. Immunoprecipitation using anti-polyhistidine antibody was carried out (*lanes 1* and *2*). Co-precipitated His-tagged PLAP-1/asporin was detected with anti-polyhistidine antibody (*upper panel*), and BMP-2 was detected with anti-BMP-2 antibody (*lower panel*). Reverse immunoprecipitation using anti-BMP-2 antibody was carried out (*lanes 3* and *4*) followed by Western blotting with anti-polyhistidine antibody (*upper panel*) or anti-BMP-2 antibody (*lower panel*).

most potent cytokines for mineralization (9). This study demonstrates that PLAP-1/asporin regulates PDL cell cytodifferentiation through BMP-2 activity, which suggests that PLAP-1/asporin is part of the negative feedback mechanism of BMP-2.

We showed that, in the adult mouse, *PLAP-1/asporin* is preferentially expressed in the periodontal ligament. The PDL is a highly vascular and cellular connective tissue that plays critical roles in mineralized tissue generation and support. The periodontal ligament is situated between the tooth and the alveolar bone, and it supports the attachment of the teeth to the alveolar bone. Furthermore mesenchymal stem cells are present in the PDL and are able to differentiate into multiple types of cells that play essential roles by responding to the mechanical forces that affect teeth and by repairing damaged matrix (24). Preferential localization of *PLAP-1/asporin* in the PDL suggests that it has different and unique roles in the homeostasis and function of the PDL.

The *in situ* hybridization analysis of *PLAP-1/asporin* in mouse embryogenesis revealed that, in the maxilla and mandible, the first expression was detected at E12.5; this was followed at E13.5 by *PLAP-1/asporin* expression in the mesenchyme lateral to Meckel cartilage (8). In the present study, we showed that *PLAP-1/asporin* expression is markedly enhanced in dental follicle cells of the developing tooth germ. During tooth germ development, progenitor cells present in the dental follicle are believed to play a central role in the formation of periodontal components such as cementum, periodontal ligament, and alveolar bone (25, 26). Taken together, PLAP-1/asporin appears to be involved in the formation of periodontal tissues during tooth development.

In this study, we established a PDL cell clone to analyze PLAP-1/asporin functions *in vitro*. PDL cells have been reported to be osteogenic in nature and to differentiate into either osteoblasts or cementoblasts depending on the need and the environment. *In vitro* maintained PDL cells obtained from rats formed mineralized nodules that were different from those formed by osteoblasts (4). It has also been shown that human PDL cells, but not gingival fibroblasts, form mineral-like nodules *in vitro* (5). However, in most of the previous studies, the PDL cells were heterogeneous cell populations. Thus, it was difficult to clarify which of the cells, alone or interacting with other cell types, were responsible for the calcified nodule formation. Our findings, obtained using PDL cell clones, further indicate that PDL cells are closely related to the osteogenic cell lineage because PDL clone cells were shown to express genes, including *Runx2*, thought to be specific to osteoblasts and to produce mineralized nodules during the cytodifferentiation process.

By using the PDL cell clones, we demonstrated that PLAP-1/asporin represses the cytodifferentiation and mineralization that occurs during the PDL differentiation process. We also found that PLAP-1/asporin negatively regulates the BMP-2-induced differentiation of PDL cells. Interestingly we demonstrated that recombinant PLAP-1/asporin directly interacts with BMP-2 *in vitro*. We also found that recombinant PLAP-1/asporin inhibits the BMP-2-induced differentiation of PDL cells (72.8% inhibition to control). These findings are supported by the previous report showing that PLAP-1/asporin suppresses chondrogenesis by inhibiting TGF-β function through a direct interaction (10). Both BMP-2 and TGF-β belong to the TGF-β superfamily and share consensus structures. TGF-β signaling is crucial for maintaining articular cartilage and for preventing osteoarthritis. On the other hand, BMP-2 plays crucial roles in bone formation and metabolism. Our findings strongly suggest that PLAP-1/asporin binds directly to BMP-2 and suppresses BMP-2 signaling in PDL tissues *in vivo*. The actual binding site of PLAP-1/asporin to BMP-2 is still unclear. However, there are some reports showing that leucine-rich repeats (LRRs), which are found in PLAP-1/asporin, are involved in protein-protein interactions and have been found in a large number of proteins, including SLRP family proteins such as decorin, biglycan, fibromodulin, and lumican (27). Decorin binds to collagen mainly through LRR-4 and -5 of the core protein (28). In addition, a high affinity binding site for TGF-β is located between LRR-3 and -5 (29).

Downloaded from www.jbc.org at OSAKA UNIVERSITY on August 7, 2007

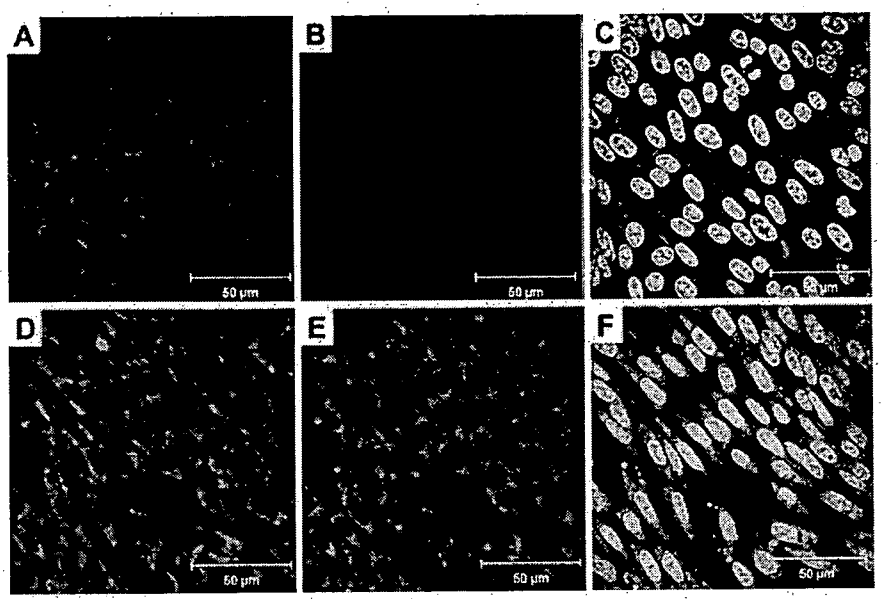

FIGURE 9. **Co-localization of PLAP-1/asporin and BMP-2.** FLAG-tagged PLAP-1/asporin-transfected MPDL22 cells were analyzed by two-color immunohistochemical staining. Transfected cells were preincubated with BMP-2 (10 μg/ml) before staining. *A–C*, mock-transfected control MPDL22 cells. *D–F*, FLAG-tagged PLAP-1/asporin-transfected MPDL22 cells. *A* and *D*, anti-BMP-2 staining (*red*). *B* and *E*, anti-FLAG staining (*green*). *C* and *F*, merged image of anti-BMP-2 and anti-FLAG staining. Nuclear staining with 4′,6-diamidino-2-phenylindole is shown in *blue*.

Decorin binding to TGF-β prevents the binding of TGF-β to its receptor and regulates TGF-β-mediated cellular signaling (30). It is also suggested that decorin interacts with vascular endothelial growth factor through LRR-5 (31). Taken together, it is quite possible that PLAP-1/asporin interacts with BMP-2 through LRRs, and we are currently conducting experiments to assess this possibility.

Decorin and biglycan show high homology and similarity to PLAP-1/asporin (6–8). Interestingly recent studies have revealed that biglycan positively modulates osteoblast differentiation and matrix mineralization by regulating BMP-4 signaling (23, 32). On the other hand, decorin has been shown to suppress osteoblast differentiation *in vitro* (33). In our study, the overexpression of PLAP-1/asporin in MC3T3-E1 preosteoblastic cells was found to inhibit osteoblast differentiation and mineralization (data not shown). These opposing effects of SLRPs on osteoblast differentiation and mineralization have not been explained. The three SLRPs have different numbers of glycosaminoglycan attachment sites. PLAP-1/asporin has no glycosaminoglycan site, whereas biglycan has two glycosaminoglycan sites, and decorin has one glycosaminoglycan site (6–8). These differences may contribute to the specific functions that the various SLRPs have in cytodifferentiation and mineralization.

Ankylosis between tooth root and alveolar bone results in pathological resorption of the tooth and bone, leading to fracture. As cited above, the PDL has a high osteogenic potential, and many PDL cells highly express Runx2 and ALPase *in vivo* (34). However, the PDL is comprised of tough yet flexible connective tissue *in vivo*. The molecular mechanism by which the PDL is maintained and not ossified has not yet been fully clarified. Msx2, which is a transcriptional factor with a homeobox domain, has recently been reported to be dominantly expressed in the PDL and to suppress PDL cytodifferentiation and mineralization through the inhibition of Runx2 functions (35). Another study revealed that S100A4, which is an intracellular calcium-binding protein, suppresses differentiation of PDL cells as well as osteoblasts (36, 37). However, the expression of these molecules is relatively ubiquitous. In contrast, *PLAP-1/asporin* showed very specific expression in limited tissue types. This supports the idea that PLAP-1/asporin, compared with other molecules, has other functions in the PDL in addition to regulating PDL cell differentiation.

In conclusion, we showed that endogenous PLAP-1/asporin may prevent the PDL from undergoing osteogenic and cementogenic processes probably by inhibiting BMP-2 functions to maintain PDL homeostasis *in vivo*. This may be the molecular mechanism by which the PDL prevents the onset of ossification despite having osteoblastic potential.

REFERENCES

1. Beertsen, W., McCulloch, C. A., and Sodek, J. (1997) *Periodontol. 2000* **13,** 20–40
2. Bartold, P. M., Shi, S., and Gronthos, S. (2006) *Periodontol. 2000* **40,** 164–172
3. Seo, B. M., Miura, M., Gronthos, S., Bartold, P. M., Batouli, S., Brahim, J., Young, M., Robey, P. G., Wang, C. Y., and Shi, S. (2004) *Lancet* **364,** 149–155
4. Cho, M. I., Matsuda, N., Lin, W. L., Moshier, A., and Ramakrishnan, P. R. (1992) *Calcif. Tissue Int.* **50,** 459–467
5. Arceo, N., Sauk, J. J., Moehring, J., Foster, R. A., and Somerman, M. J. (1991) *J. Periodontol.* **62,** 499–503
6. Yamada, S., Murakami, S., Matoba, R., Ozawa, Y., Yokokoji, T., Nakahira, Y., Ikezawa, K., Takayama, S., Matsubara, K., and Okada, H. (2001) *Gene (Amst.)* **275,** 279–286
7. Lorenzo, P., Aspberg, A., Onnerfjord, P., Bayliss, M. T., Neame, P. J., and Heinegard, D. (2001) *J. Biol. Chem.* **276,** 12201–12211
8. Henry, S. P., Takanosu, M., Boyd, T. C., Mayne, P. M., Eberspaecher, H., Zhou, W., de Crombrugghe, B., Hook, M., and Mayne, R. (2001) *J. Biol. Chem.* **276,** 12212–12221
9. Yamada, S., Ozawa, Y., Tomoeda, M., Matoba, R., Matsubara, K., and Murakami, S. (2006) *J. Dent. Res.* **85,** 447–451
10. Kizawa, H., Kou, I., Iida, A., Sudo, A., Miyamoto, Y., Fukuda, A., Mabuchi, A., Kotani, A., Kawakami, A., Yamamoto, S., Uchida, A., Nakamura, K., Notoya, K., Nakamura, Y., and Ikegawa, S. (2005) *Nat. Genet.* **37,** 138–144
11. Iida, A., Kizawa, H., Nakamura, Y., and Ikegawa, S. (2006) *J. Hum. Genet.* **51,** 151–154
12. Ikegawa, S., Kawamura, S., Takahashi, A., Nakamura, T., and Kamatani, N. (2006) *Arthritis Res. Ther.* **8,** 403
13. Toyosawa, S., Shintani, S., Fujiwara, T., Ooshima, T., Sato, A., Ijuhin, N., and Komori, T. (2001) *J. Bone Miner. Res.* **16,** 2017–2026
14. Reynolds, A., Leake, D., Boese, Q., Scaringe, S., Marshall, W. S., and Khvorova, A. (2004) *Nat. Biotechnol.* **22,** 326–330
15. Bessey, O., Lowry, O., and Brock, M. (1946) *J. Biol. Chem.* **164,** 321–329
16. Dahl, L. K. (1952) *Proc. Soc. Exp. Biol. Med.* **80,** 474–479
17. Labarca, C., and Paigen, K. (1980) *Anal. Biochem.* **102,** 344–352

Downloaded from www.jbc.org at OSAKA UNIVERSITY on August 7, 2007

18. Ishihara, K., Satoh, I., Nittoh, T., Kanaya, T., Okazaki, H., Suzuki, T., Koyama, T., Sakamoto, T., Ide, T., and Ohuchi, K. (1999) *Biochim. Biophys. Acta* **1451**, 48–58
19. Hogan, B. L. (1996) *Curr. Opin. Genet. Dev.* **6**, 432–438
20. Kobayashi, M., Takiguchi, T., Suzuki, R., Yamaguchi, A., Deguchi, K., Shionome, M., Miyazawa, Y., Nishihara, T., Nagumo, M., and Hasegawa, K. (1999) *J. Dent. Res.* **78**, 1624–1633
21. Zhao, M., Xiao, G., Berry, J. E., Franceschi, R. T., Reddi, A., and Somerman, M. J. (2002) *J. Bone Miner. Res.* **17**, 1441–1451
22. Hildebrand, A., Romaris, M., Rasmussen, L. M., Heinegard, D., Twardzik, D. R., Border, W. A., and Ruoslahti, E. (1994) *Biochem. J.* **302**, 527–534
23. Chen, X. D., Fisher, L. W., Robey, P. G., and Young, M. F. (2004) *FASEB J.* **18**, 948–958
24. Lekic, P., and McCulloch, C. A. (1996) *Anat. Rec.* **245**, 327–341
25. Bosshardt, D. D., and Schroeder, H. E. (1996) *Anat. Rec.* **245**, 267–292
26. Saito, M., Handa, K., Kiyono, T., Hattori, S., Yokoi, T., Tsubakimoto, T., Harada, H., Noguchi, T., Toyoda, M., Sato, S., and Teranaka, T. (2005) *J. Bone Miner. Res.* **20**, 50–57
27. Matsushima, N., Ohyanagi, T., Tanaka, T., and Kretsinger, R. H. (2000) *Proteins* **38**, 210–225
28. Svensson, L., Heinegard, D., and Oldberg, A. (1995) *J. Biol. Chem.* **270**, 20712–20716
29. Schonherr, E., Broszat, M., Brandan, E., Bruckner, P., and Kresse, H. (1998) *Arch. Biochem. Biophys.* **355**, 241–248
30. Stander, M., Naumann, U., Wick, W., and Weller, M. (1999) *Cell Tissue Res.* **296**, 221–227
31. Sulochana, K. N., Fan, H., Jois, S., Subramanian, V., Sun, F., Kini, R. M., and Ge, R. (2005) *J. Biol. Chem.* **280**, 27935–27948
32. Parisuthiman, D., Mochida, Y., Duarte, W. R., and Yamauchi, M. (2005) *J. Bone Miner. Res.* **20**, 1878–1886
33. Mochida, Y., Duarte, W. R., Tanzawa, H., Paschalis, E. P., and Yamauchi, M. (2003) *Biochem. Biophys. Res. Commun.* **305**, 6–9
34. Saito, Y., Yoshizawa, T., Takizawa, F., Ikegame, M., Ishibashi, O., Okuda, K., Hara, K., Ishibashi, K., Obinata, M., and Kawashima, H. (2002) *J. Cell Sci.* **115**, 4191–4200
35. Yoshizawa, T., Takizawa, F., Iizawa, F., Ishibashi, O., Kawashima, H., Matsuda, A., Endo, N., and Kawashima, H. (2004) *Mol. Cell. Biol.* **24**, 3460–3472
36. Duarte, W. R., Shibata, T., Takenaga, K., Takahashi, E., Kubota, K., Ohya, K., Ishikawa, I., Yamauchi, M., and Kasugai, S. (2003) *J. Bone Miner. Res.* **18**, 493–501
37. Duarte, W. R., Iimura, T., Takenaga, K., Ohya, K., Ishikawa, I., and Kasugai, S. (1999) *Biochem. Biophys. Res. Commun.* **255**, 416–420

Downloaded from www.jbc.org at OSAKA UNIVERSITY on August 7, 2007

Available online at www.sciencedirect.com
ScienceDirect
Matrix Biology 27 (2008) 232–241
MATRIX BIOLOGY
www.elsevier.com/locate/matbio

Basic fibroblast growth factor regulates expression of heparan sulfate in human periodontal ligament cells

Yoshio Shimabukuro, Tomoo Ichikawa, Yoshimitsu Terashima, Tomoaki Iwayama, Hiroyuki Oohara, Tetsuhiro Kajikawa, Ryohei Kobayashi, Hiroaki Terashima, Masahide Takedachi, Mami Terakura, Tomoko Hashikawa, Satoru Yamada, Shinya Murakami *

Department of Periodontology, Division of Oral Biology and Disease Control, Osaka University Graduate School of Dentistry, 1-8 Yamadaoka, Suita, Osaka 565-0871, Japan

Received 30 March 2006; received in revised form 25 September 2007; accepted 19 October 2007

Abstract

Heparan sulfate (HS) proteoglycan is a widely distributed biological molecule that mediates a variety of physiological responses in development, cell growth, cell migration, and wound healing. We examined the effects of basic fibroblast growth factor-2 (FGF-2), which is known to modulate extracellular matrix (ECM) production of various cell types, on the production of HS proteoglycan by human periodontal ligament (HPDL) cells. We also examined the effects of FGF-2 on the expression of syndecans, a major family of membrane-bound HS proteoglycans. Treatment of HPDL cells with FGF-2 for 72 h resulted in a pronounced increase in the level of HS in the culture supernatant in a dose-dependent manner. However, reverse transcription-polymerase chain reaction data (RT-PCR) revealed that FGF-2 marginally reduced the gene expression of syndecan-1, -2, and -4, and did not alter the level of syndecan-3 mRNA. Furthermore, FGF-2 did not have an effect on the mRNA expression of enzymes associated with HS biosynthesis. Interestingly, FACS analysis revealed that the syndecan family displayed diverse alterations in response to FGF-2. FGF-2 barely altered the expression of syndecan-1, but decreased the expression of syndecan-2 and -4 on HPDL cells. Moreover, dot blot analysis showed that FGF-2 did not alter the level of syndecan-1 and -2, but enhanced the level of syndecan-4 in culture supernatants of FGF-2-stimulated HPDL cells. These results suggest that the FGF-2-activated increase in the level of HS in conditioned medium may be a result of shedding of syndecan-4 from the HPDL cell surface. Taken together, FGF-2 may differentially regulate the expression of HS proteoglycans in a HS-proteoglycan-subtype-dependent manner. The diversity of the expression patterns of HS proteoglycans may be associated with the FGF-2-induced biological functions of HPDL cells.
© 2007 Elsevier B.V./International Society of Matrix Biology. All rights reserved.

Keywords: Basic fibroblast growth factor; Heparan sulfate; Periodontal ligament cells; Shedding; Syndecan

1. Introduction

A wide range of extracellular matrix and growth factors participate during the wound-healing process. The basic fibroblast growth factor-2 (FGF-2) is one such growth factor detected in the early phase of wound healing. FGF-2 mediates various biological responses including cellular proliferation, angiogenesis, and tissue repair (Bikfalvi et al., 1997; Nugent and Iozzo, 2000). FGF-2 also modulates the expression of glycosaminoglycans and proteoglycans, as well as collagen and non-collagenous protein, which are main components of connective tissue. However, the details of the regulatory effects of FGF-2 on the expression of glycosaminoglycans and proteoglycans in cells have not been fully defined.

The syndecans are a family of cell surface heparan sulfate (HS) proteoglycans which comprise of a core protein and glycosaminoglycan side chains. Four members of the syndecan family have been identified to date. Whereas syndecan-4 expression is ubiquitous, syndecan-1, -2, and -3 are mainly present in epithelial cells, fibroblasts, and neural cells, respectively. The HS chains of the syndecans are responsible for their biological

* Corresponding author. Tel.: +81 6 6879 2930; fax: +81 6 6879 2934.
E-mail address: ipshinya@dent.osaka-u.ac.jp (S. Murakami).

0945-053X/$ - see front matter © 2007 Elsevier B.V./International Society of Matrix Biology. All rights reserved.
doi:10.1016/j.matbio.2007.10.005

functions, such as extracellular matrix assembly and growth factor binding. The HS chains of syndecans are also known to function as co-receptors of the FGF receptor. It has been reported that when tissue was injured, syndecan expression was increased in epithelial cells, endothelial cells, and fibroblasts (Elenius et al., 1997; Gallo et al., 1996), and shed syndecan ectodomain accumulated in wound fluid (Fitzgerald et al., 2000; Kainulainen et al., 1998; Park et al., 2000). Recent studies have also revealed impaired wound healing in syndecan-deficient mice (Echtermeyer et al., 2001; Ishiguro et al., 2000; Stepp et al., 2002), suggesting an essential role for the syndecans in wound repair.

Periodontal tissue is a tooth-supporting tissue and consists of periodontal ligament, gingiva, cementum, and alveolar bone. The periodontal ligament cells have the potential to secrete a variety of extracellular matrices and support teeth with these molecules. Furthermore, they play key roles in regeneration events following periodontal tissue breakdown caused by progression of periodontal diseases. Interestingly, we revealed that topical application of FGF-2 to periodontal tissue defects activates regeneration of tissue with new cementum and ligament tissue formation (Murakami et al., 1999), which may be a result of FGF-2 increasing cell growth and modulating extracellular matrices. In addition, we explained the stimulatory effects of FGF-2 on the expression of the high molecular type of hyaluronan, a non-sulfated glycosaminoglycan, by human periodontal ligament (HPDL) cells via the up-regulation of hyaluronan synthase (HAS)1 and HAS2 (Shimabukuro et al., 2005). Here we examined the production of HS and the expression pattern of the syndecan gene family by HPDL cells in response to FGF-2.

2. Experimental procedures

2.1. Reagent

Human recombinant FGF-2 was provided by Kaken Pharmaceutical Co., Ltd. (Tokyo, Japan).

2.2. HPDL cells

HPDL cells were isolated from healthy periodontal ligaments of first premolar teeth of individuals undergoing tooth extraction for orthodontic treatment in accordance with the method of Somerman et al. (1988), with minor modifications. All the patients gave informed consent before providing the samples. Healthy periodontal tissue was removed from the center of the root surface with a surgical scalpel. The tissue was minced then transferred to Leighton tubes (Costor, Cambridge, MA, USA). The explants were cultured in α-MEM supplemented with 10% FCS, 50 U/ml penicillin G, and 50 μg/ml streptomycin (henceforth denoted standard medium), with medium changed every 2 or 3 days. Cells were cultured at 37 °C in a humidified atmosphere of 95% air and 5% CO_2. When the cells growing out from the explants had reached confluence, they were separated by treatment with a solution containing 0.05% trypsin and 0.53 mM ethylenediaminetetraacetic acid, collected by centrifugation, and cultured in standard medium in culture dishes until confluency. The cells were then trypsinized and split at a 1:3 ratio. Experiments were carried out with cells from the fourth to fifth passages. In this study, we established 3 cell lines from different volunteers, and all cell lines were used in each experiment. All these cell lines provided similar results in each experiment of this study.

2.3. Reverse transcription-polymerase chain reaction (RT-PCR) for quantitation of mRNA levels

HPDL cells were seeded at a density of 10^5 cells/dish in 600-mm dishes and grown to confluency in standard medium. Following 24 or 48 hours of activation in the absence or presence of FGF-2 (50 ng/ml), total RNA was isolated from HPDL cells by RNAzol™ (Cinna/Biotecx Laboratories Inc., Friendswood, TX, USA), according to the manufacturer's instructions. The precipitated RNA was resuspended in 0.1% diethylpyrocarbonate-treated distilled water (DEPC-treated H_2O). This RNA sample was heatdenatured at 65 °C for 10 min and chilled on ice. Complementary DNA (cDNA) synthesis and amplification via PCR were performed as described previously. cDNA synthesis was carried out in a 40 μl reverse transcription mixture containing 52.5 mM Tris–HCl; pH 8.3, 75.5 mM KCl, 3 mM $MgCl_2$, 0.5 mM each dNTPs, 1 mM dithiothreitol, 1.1 U/μl RNase inhibitor (Takara Biomedicals, Shiga, Japan), 55 ng/μl random hexamer, 5 U/μl M-MLV reverse transcriptase (Gibco, Gaithersburg, MD, USA) and RNA. The mixture was incubated at 37 °C for 60 min. At the end of the reverse transcription, all samples were heated at 99 °C for 5 min to inactivate the enzyme and were diluted into 110 μl of DEPC-treated H_2O.

Oligonucleotide PCR primers specific for HS biosynthesis-related enzymes, syndecan-1, -2, -3, and -4, and hypoxanthine phosphoribosyl transferase (HPRT) were synthesized at Takara Shuzo Co. Ltd. (Table 1).

Table 1
Primers utilized for reverse transcription-polymerase chain reaction

Primers	Size		Sequence
HPRT	303 bp	Sense	5′CGAGATGTGATGAAGGAGATGGG3′
		Antisense	5′GCCTGACCAAGGAAAGCAAAGTC3′
GlcNAcT-1	546 bp	Sense	5′CTAAGCTGCAGGGAAATAAA3′
		Antisense	5′TTGCTGTCTGTTGTTTGAAG3′
HS2ST	443 bp	Sense	5′AGGATTTTATCATGGACACG3′
		Antisense	5′TCTTTCCTGTGCGATAGAGT3′
NDST-1	450 bp	Sense	5′ATCTTCTGCCTGTTCAGCGT3′
		Antisense	5′CTCATTGGCCTTGAAGAAGC3′
NDST-2	580 bp	Sense	5′CATGAAGGTGGCTGAGTTG3′
		Antisense	5′CGGATTAAGCAGCACTGTCA3′
Epimerase	624 bp	Sense	5′AGGTGGTTAGGTTGATTGCG3′
		Antisense	5′GCAGTTGATTGATGTGGGTG3′
Syndecan-1	472 bp	Sense	5′CTTTGAAACCTCGGGGAGAATAC3′
		Antisense	5′TCCAGGCAGAAGTCAGAGAAGCAG3′
Syndecan-2	395 bp	Sense	5′GGAGCTGATGAGGATGTAGA3′
		Antisense	5′CACTGGATGGTTTGCGTTCT3′
Syndecan-3	292 bp	Sense	5′GCTTCTTTTCCCTTTTACCCTCCGC3′
		Antisense	5′TGTTCCCCAACTTCTCTCTGCCAAG3′
Syndecan-4	245 bp	Sense	5′GGGCAGGAATCTGATGACTTTGAG3′
		Antisense	5′GCTGGACATTGACACCTTGTTGC3′

PCR was performed in a 50 μl mixture containing 5 μl of each sample of derived cDNA, 10 mM Tris–HCl; pH 8.3, 50 mM KCl, 1.5 mM $MgCl_2$, 0.15 mM of each dNTP, 1.25 mM Ampli Taq Gold™ (Perkin Elmer Cetus Co., Emeryville, CA, USA) and 0.2 mM of each primer. After 9 min of predenaturation at 94 °C, PCR was performed in a DNA thermal cycler (MJ Research Inc., Watham, MA, USA) for 21, 24, 27, 30, 33 and 36 cycles to optimize the cycle number to maintain exponential conditions of amplification. Each cycle consisted of denaturation at 94 °C for 45 s, annealing at 56 °C for 45 s, polymerization at 72 °C for 90 s. The 7 μl samples were analyzed on 2% agarose ethidium bromide gels run at 100 V for 25–30 min.

2.4. Determination of the level of HS in culture supernatants

HPDL cells were seeded at a density of 5×10^5 cells in 100-mm culture dishes (Corning Laboratory Sciences Company, Corning, NY, USA) and grown in standard medium. When the monolayers were confluent, the cells were rinsed twice with Hanks' balanced salt solution and incubated in 10% FCS-αMEM in the absence or presence of FGF-2 (1–50 ng/ml). At the end of the incubation periods, the supernatants were collected and stored at −20 °C until determination of HS levels. The HS levels in culture supernatants were measured by an enzyme-linked immunosorbent assay (HS assay kit, Seikagaku Co., Tokyo, Japan), following the manufacturer's instructions. Samples or HS standards were added to the wells which were coated with an anti-HS antibody, and incubated at 4 °C for 24 h. After washing, bound HS was detected by incubating with a biotinylated-antibody specific for HS and horse radish peroxidase (HRP)-conjugated streptavidin for 1 h at room temperature. The plates were washed, loaded with 3,3′,5,5′-tetramethylbenzidene substrate solution and incubated at room temperature before the reaction was stopped with stop solution. Absorbance was measured by a microplate reader (MTP-32; Corona Electric, Hitachinaka, Japan) set at 450 nm/630 nm. The HS levels in samples were calculated from the HS standard curve.

In order to determine the optimal dose of each cytokine for comparison in this study, we preliminarily examined the proliferative responses of HPDL cells induced by the cytokines. A non-saturating dose, which induced nearly equal responses among the cytokines, was selected as an optimal dose of each cytokine in this study. The doses for comparison of FGF-2, epidermal growth factor (EGF), hepatocyte growth factor (HGF), insulin like growth factor-1 (IGF-1), platelet-derived growth factor-BB (PDGF-BB), and transforming growth factor-β (TGF-β) were 50, 100, 50, 50, 50, and 10 ng/ml, respectively.

2.5. Immunocytochemical analysis

HPDL cells were seeded at a density of 5×10^3 cells in 35-mm glass bottom dishes (Matsunami Glass Ind. Ltd., Kishiwada, Japan) and cultured until confluency. At the time of the assay, culture medium was replaced with fresh medium, supplemented with 10% FCS, in the absence or presence of FGF-2 (50 ng/ml). Cells were cultured at 37 °C for the indicated times.

Cell monolayers were fixed with acetone or 2% paraformaldehyde for 10 min, then blocked with 1% bovine serum albumin (BSA) and 10% goat serum in PBS at room temperature for 30 min. The primary antibodies used were: mouse anti-human syndecan-1 antibody (Serotec Ltd., Kidlington, Oxford, UK); goat anti-human syndecan-2 antibody (Santa Cruz Biotechnology Inc., Santa Cruz, California, USA); goat anti-syndecan-4 antibody (Santa Cruz Biotechnology Inc.); mouse monoclonal biotinylated anti-hyaluronan antibody (10E4; Seikagaku Co.). Monolayers were washed three times with PBS to remove unbound antibody, then incubated for 30 min at 37 °C with Alexa Fluor 488-labeled polyclonal anti-mouse or goat IgG antibodies (Molecular Probes, Carlshad, CA, USA) or Alesa Fluor 568-labeled streptavidin (Molecular Probes). The samples were mounted on coverslipped, then viewed using an OLYMPUS 1×70 microscope (Tokyo, Japan) and photographed.

2.6. FACS analysis

HPDL cells were incubated in 10% FCS-αMEM in the absence or presence of FGF-2 (50 ng/ml). At the time of the assay, cells were incubated with mouse anti-human syndecan-1 antibody (Serotec Ltd.), goat anti-human syndecan-2 antibody (Santa Cruz Biotechnology Inc.), and biotin-conjugated mouse anti-syndecan-4 antibody (Santa Cruz Biotechnology Inc.) as primary antibodies. The cells were washed three times with PBS and incubated for 30 min at 37 °C with or without FITC-labeled polyclonal anti-mouse antibody (Caltag Laboratories, Burlingame, CA, USA),

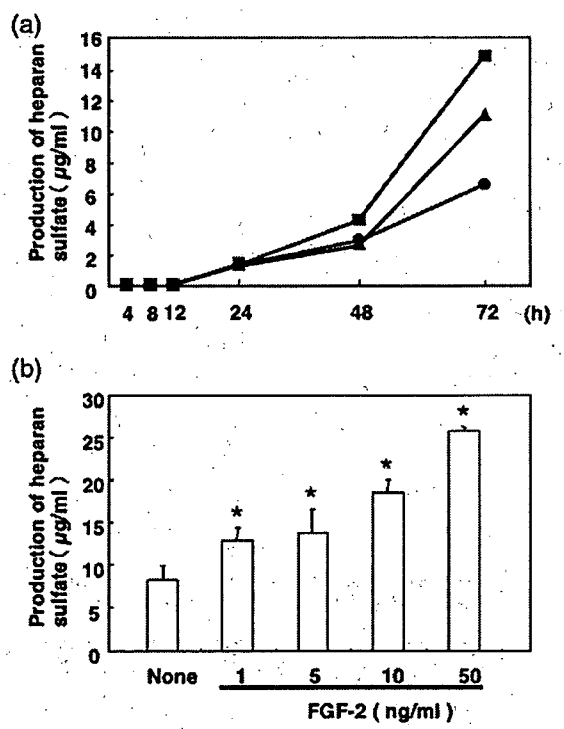

Fig. 1. Effect of FGF-2 on the production of HS by HPDL cells. HPDL cells were cultured in the absence (●) or presence of FGF-2 (5: ▲, 50: ■ ng/ml) and cultured for the indicated times (a.). HPDL cells were cultured in the absence or presence of FGF-2 (1, 5, 10, 50 ng/ml) for 72 h (b.). Conditioned medium was removed and the level of HS analyzed using an enzyme-linked immunosorbent assay. Results of one representative experiment from three separate experiments are shown. (*$p<0.05$ compared to unstimulated control).

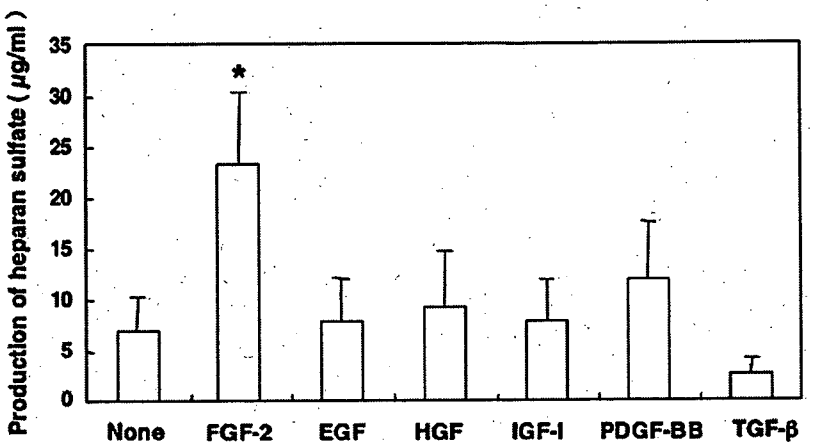

Fig. 2. Effect of various cytokines on HS production by HPDL cells. HPDL cells were cultured without any cytokine or with FGF-2 (50 ng/ml), EGF (100 ng/ml), HGF (50 ng/ml), IGF-1 (50 ng/ml), PDGF-BB (50 ng/ml), or TGF-β (10 ng/ml). Culture supernatants were removed after 72 h of exposure to the various cytokines, and the HS concentration measured by enzyme-linked immunosorbent assay. Results of one representative experiment from three separate experiments are shown. (*$p<0.05$ compared to unstimulated control).

FITC-labeled polyclonal anti-goat antibody (Santa Cruz Biotechnology Inc.), or FITC-labeled streptavidin (BD Biosciences, San Diego, CA).

2.7. Dot blot analysis

Medium from FGF-2-stimulated or unstimulated HPDL cells was collected, and a 400-μl sample spotted onto a nitrocellulose membrane. The membrane was blocked for 1 h with PBS containing 10% BSA, incubated overnight at 4 °C with a mouse monoclonal antibody to syndecan-1, -2, or -4, or a goat polyclonal antibody to glypican-1 (Santa Cruz), -2 (R&D Systems, Inc., Minneapolis, MN, USA), -3 (Santa Cruz), -6 (R&D Systems, Inc.), or perlecan (Santa Cruz), washed with PBS containing 1% BSA, and then incubated with HRP-conjugated rabbit anti-mouse serum or anti-goat serum. Immunoreactive bands were identified using a chemiluminescent kit (ECL, Amersham Pharmacia Biotech, Piscataway, NJ, USA), and were scanned densitometrically and analyzed using NIH image 1.63.

2.8. Statistical analysis

Data are expressed as mean ± standard deviation, and were compared by ANOVA and *post-hoc* Scheffé's comparisons.

3. Results

3.1. FGF-2 induced production of HS by HPDL cells, but did not affect the production of HS biosynthesis-associated enzymes

Although FGF-2 has been reported to modulate extracellular matrix production, the effects of FGF-2 on glycosaminoglycan production by HPDL cells have not been fully elucidated (Shimabukuro et al., 2005). Focusing on HS production by HPDL cells, we first analyzed the concentration of HS in conditioned medium of FGF-2-stimulated HPDL cells. HS (1.29 μg/ml) was detected in the culture supernatants after 24 h of stimulation. The concentration of HS was found to gradually increase during 72 h of stimulation, with the increase

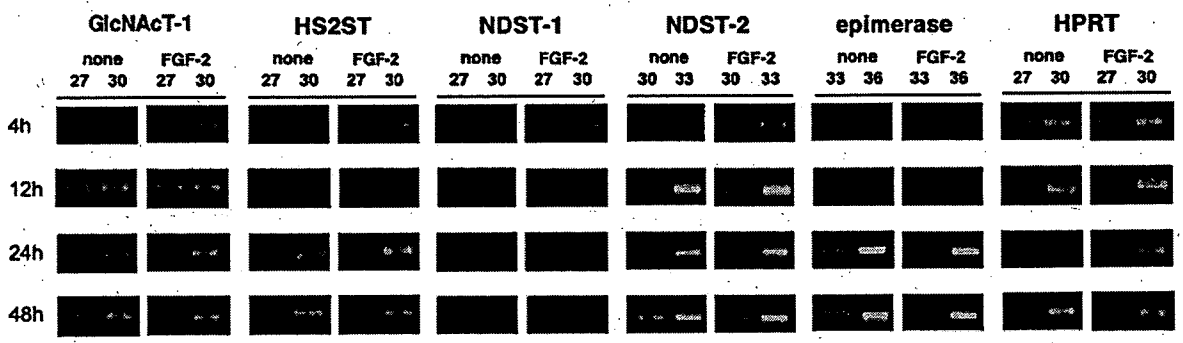

Fig. 3. mRNA expression of HS synthetic enzymes in HPDL cells. The expression of mRNA of HS-related enzymes in HPDL cells cultured in the absence or presence of FGF-2 (50 ng/ml) for 24 h was measured. Total RNA was recovered and RT-PCR performed to analyze the mRNA expression of GlcNAcT-1, HS2ST, NDST-1, NDST-2, epimerase, and HPRT in HPDL cells. Results of one representative experiment from three separate experiments are shown. The number of PCR amplification cycles is shown above each lane.

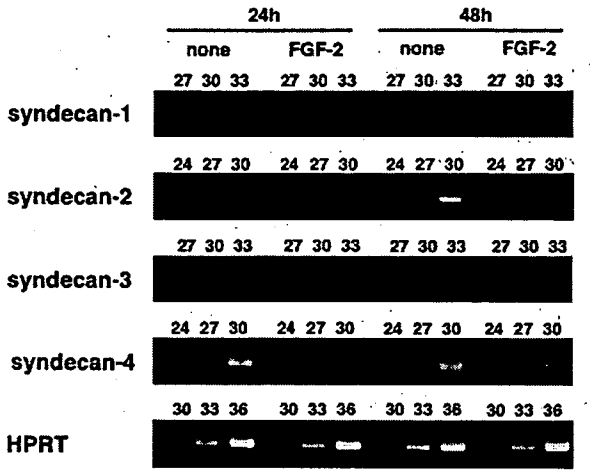

Fig. 4. mRNA expression of the syndecan gene family in HPDL cells. The expression of mRNA of the syndecan gene family in HPDL cells cultured in the absence or presence of FGF-2 (50 ng/ml) for 24 h and 48 h was measured. Total RNA was recovered and RT-PCR performed to analyze the mRNA expression of syndecan-1, -2, -3, and -4, and HPRT in HPDL cells. Results of one representative experiment from three separate experiments are shown. The number of PCR amplification cycles is shown above each lane.

between 48 and 72 h being particularly pronounced. In addition, the amount of HS produced was dependent on the dose of FGF-2 (Fig. 1).

The effects of other cytokines on the production of HS were then investigated, as production of HS can be modulated by various factors. In contrast to the marked effect of FGF-2, PDGF-BB slightly stimulated and TGF-β weakly suppressed the production of HS by HPDL cells, and the other cytokines examined (EGF, HGF, and IGF-1) did not alter HS production (Fig. 2). However, minor effects of PDGF-BB and TGF-β were not statistically significant.

HS synthesis is extended with *N*-acetyl-glucosamine (GlcNAc) from the four initial monosaccharides, and the growing glycosaminoglycan chains are modified by epimerazation, deacetylation/*N*-sulfation, and *O*-sulfation (Prydz and Dalen, 2000). Thus, we used semi-quantitative RT-PCR to examine the gene expressions of enzymes involved in the biosynthesis of HS 4, 12, 24 and 48 h after FGF-2 stimulation. However, we found that gene expressions of *N*-acetylglucosaminyltransferase (GlcNAcT)-1, heparan sulfate 2-*O*-sulfotransferase (HS2ST), *N*-deacetylase/*N*-sulfotransferase (NDST)-1, NDST-2, epimerase,

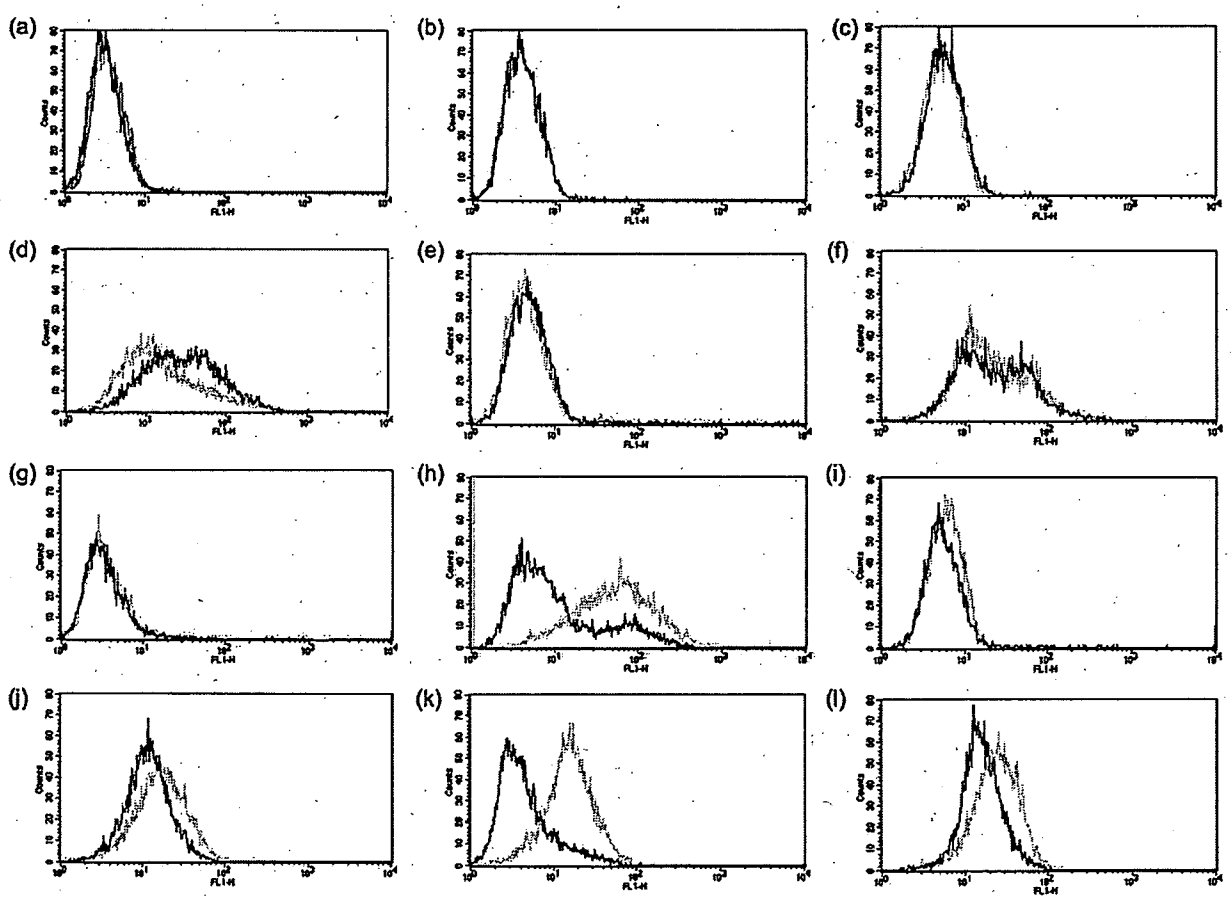

Fig. 5. FACS analysis of syndecan expression on HPDL cells. HPDL cells were incubated in 10% FCS-αMEM in the absence (gray line) or presence of FGF-2 (50 ng/ml) (black line) for 24 h (a, d, g, j), 48 h (b, e, h, k) or 72 h (c, f, i, l). At the time of the assay, cells were incubated without (a, b, c) or with the following primary antibodies: mouse anti-human syndecan-1 antibody (d, e, f); goat anti-human syndecan-2 antibody (g, h, i); mouse anti-syndecan-4 antibody (j, k, l). The cells were washed three times with PBS and incubated for 30 min at 37 °C with or without a biotinylated polyclonal anti-mouse or anti-goat antibody. After washing with PBS, staining was achieved with streptavidin-FITC.